

The 5-Electron case of Thomson's Problem

Richard Evan Schwartz *

October 30, 2018

Abstract

We give a rigorous, computer-assisted proof that the triangular bi-pyramid is the unique configuration of 5 points on the sphere that globally minimizes the Coulomb ($1/r$) potential. We also prove the same result for the ($1/r^2$) potential. The main mathematical contribution of the paper is a fairly efficient energy estimate that works for any number of points and any power law potential.

1 Introduction

1.1 Background

The problem of finding how electrons optimally distribute themselves on the sphere is a well-known and difficult one. It is known as *Thomson's problem*, and dates from J. J. Thomson's 1904 publication [T]. Thomson's problem is of interest not just to mathematicians, but also to physicists and chemists.

Here is a mathematical formulation. Let $S^2 \subset \mathbf{R}^3$ be the unit sphere. Let P be a collection of n distinct point $p_1, \dots, p_n \in S^2$. Let $E : \mathbf{R}^+ \rightarrow \mathbf{R}^+$ be some function. the total energy to be the sum

$$\mathcal{E}(P) = \sum_{i>j} E(\|p_i - p_j\|). \quad (1)$$

Here $\|\cdot\|$ is the usual norm on \mathbf{R}^3 , and $\|p_i - p_j\|$ is the distance from p_i to p_j . The question is then: What does P look like if $\mathcal{E}(P)$ is as small as possible?

* Supported by N.S.F. Research Grant DMS-0072607

The question is perhaps too broad as stated, because the answer likely depends on the function E . To consider a narrower question, one restricts the class of functions in some way. For instance, a natural class of potential functions is given by the *power laws*

$$E(r) = \frac{1}{r^e}; \quad e \in (0, \infty). \quad (2)$$

The case $e = 1$ is specially interesting to physicists. It is known as the *Coulomb potential*. When energy is measured with respect to the Coulomb potential, the points are naturally considered to be electrons.

There is a large literature on Thomson's problem. One early work on Thomson's problem is [C]. The paper [SK] gives a nice survey in the two dimensional case, with an emphasis on the case when n is large. The paper [BBCGKS] gives a survey of results, both theoretical and experimental, about highly symmetric configurations in higher dimensions. The fairly recent paper [RZS] has some theoretical bounds for the logarithmic potential, and also has a large amount of experimental information about configurations minimizing the power laws on the 2-sphere. The website [CCD] has a list of experimentally determined (candidate) minimizers for the Coulomb potential for $n = 2, \dots, 972$.

There are certain values of n where the minimal configuration is rigorously known for all the power laws.

- When $n = 2$, the points of P are antipodal.
- When $n = 3$, the points of P make an equilateral triangle in an equator.
- When $n = 4$, the points of P are the vertices of a regular tetrahedron.
- When $n = 6$, the points of P are the vertices of a regular octahedron.
- When $n = 12$, the points of P are the vertices of a regular icosahedron.

The cases $n = 2$ is trivial to prove, and the case $n = 3$ is an easy exercise. The cases $n = 4, 6, 12$ are all covered in [CK, Theorem 1.2], a much broader result concerning a fairly general kind of energy potential and a class of point configurations (not restricted to 2 dimensions) called *sharp configurations*. For the specific cases cases $n = 4, 6$ see the older work [Y].

The case $n = 5$ is conspicuously absent from the above list of known results. Everyone agrees, based on numerical simulation, that the triangular

bi-pyramid (TBP) seems to be the global minimizer for the Coulomb potential. In the TBP, two points are antipodal points on S^2 and the remaining 3 points form an equilateral triangle on the equator midway between the two antipodal points. More generally, numerical experiments ¹ suggest the following.

- The TBP is a local minimizer for the power law potential with exponent e if and only if $e \in (0, e_1)$, with $e_1 \approx 21.147123$.
- The TBP is a global minimizer for the power law potential with exponent e if and only if $e \in (0, e_2)$, with $e_2 \approx 15.040808$.

For $e > e_2$, it seems that the global minimizer is a pyramid with square base. The precise configuration depends on e in this range.

In spite of detailed experimental knowledge about the case $n = 5$, it seems there has not ever been a proof that the TBP is global minimum for any power law potential. In particular, this has not been proved for the Coulomb potential. As far as we know, there are two rigorous results for the case $n = 5$.

- The paper [DLT] contains a (traditional) proof that the TBP maximizes the geometric mean of the pairwise distances between the points. This case corresponds to the logarithmic potential $E(r) = -\log(r)$.
- The paper [HS] contains a computer-aided proof that the TBP *maximizes* the potential for the exponent $e = -1$. That is, 5 points on the sphere arrange themselves into a TBP so as to maximize the total sum of the pairwise distances.

1.2 Results

It is the purpose of this paper to prove the following result.

Theorem 1.1 *The TBP is the unique configuration of minimal energy with respect to the Coulomb potential.*

Our proof is computer aided, and similar in spirit to [HS]. While the argument in [HS] is exactly tailored to understanding the sums of the distances, our method is rather insensitive to the precise power law being used. Just to illustrate this fact, we prove

¹Lacking a handy reference for these experiments, we performed our own.

Theorem 1.2 *The TBP is the unique configuration of minimal energy with respect to the $1/r^2$ potential.*

We could certainly add other exponents to our list of results. However, we currently have implemented the interval arithmetic in such a way that it works just for the exponents $e = 1, 2$. We did this to avoid using the pow function $\text{pow}(a, b) = a^b$, which is not covered by the same guarantees in the IEEE standards as are the basic arithmetic operations. See [I] and [I2]. Mainly what stops us is a sense of diminishing returns.

However, with a view towards an eventually broader application, we try to state as many estimates as we can for the general power law. In every situation, we try to point out the exact generality with which the construction holds. For example, our main technical result, Theorem 5.1, holds for any function E satisfies the conditions discussed in §5.2. Also, the version of Theorem 5.1 we prove works for general n -point configurations.

1.3 Outline of the Proof

It has probably been clear for a long time that one could prove a result like Theorem 1.1 using a computer program. The main difficulties are technical rather than conceptual. The hard part is getting estimates that are sharp enough so as to lead to a feasible calculation. Our paper doesn't really have any dramatic new ideas. It just organizes things well enough to get the job done.

We begin by eliminating some obviously bad configurations from consideration. For example we show that no two points in a minimizing configuration lie within $1/2$ units of each other. This result holds for any power law potential. See Lemma 2.1. After eliminating these bad configurations, we are left with a compact configuration space Ω of possible minimizers.

We use stereographic projection to transfer the configurations on S^2 to configurations in $\mathbf{C} \cup \infty$. By keeping one point at ∞ and another on the positive real axis, we end up with a natural description of Ω as the set $[0, 4] \times [-2, 2]^6 \subset \mathbf{R}^7$. Working in Ω , we define a natural way to subdivide a rectangular solid subset of Ω into smaller rectangular solids.

We use a divide-and-conquer algorithm to show that any minimizing configuration in Ω must lie very close to the TBP. Assuming that \mathcal{Q} is a rectangular solid that does not lie too close to the point(s) of Ω representing the TBP, we try to eliminate \mathcal{Q} with a 3-step procedure.

- We eliminate \mathcal{Q} if we can see, based on the fact that the regular tetrahedron minimizes energy for 4 points, that no configuration in \mathcal{Q} can minimize energy. This is described in §3.4. This method of eliminating \mathcal{Q} cuts away a lot of the junk, so to speak, and focuses our attention on the configurations where are fairly near the TBP.
- We eliminate \mathcal{Q} if the configurations in it are redundant, in the sense that some permutation of the vertices or obvious application of symmetry changes these configurations to ones in a form that we deem more standard. See §4.
- If the first two methods fail, we evaluate the energy \mathcal{E} on the vertices of \mathcal{Q} and then apply an *a priori* estimate on how far \mathcal{E} differs from a linear function on \mathcal{Q} . Our main result along these lines is Theorem 5.1. This is our most powerful and general method of elimination, but we only use it when all else fails.

If it is not possible to eliminate \mathcal{Q} by any of our methods, we subdivide \mathcal{Q} into smaller rectangular solids and try again on each piece. This algorithm is discussed, in outline, in §2.5. In the chapters following §2.5, we fill in the details. Theorem 5.1 is the most subtle and important part of the paper. We prove this result in §5-8.

The end result of our finite calculation is that the true minimizer of \mathcal{Q} must lie very close to the TBP. See Lemma 2.3. To finish the proof, we use calculus to show that the TPB can be the only local minimum in the region where we have confined the minimizer. We do this by showing that the Hessian of \mathcal{E} , the matrix of second partials, is positive definite throughout the region of interest to us. See Lemma 2.4.

1.4 Computational Issues

We implement our computer program in Java, using interval arithmetic to control the round-off errors. We will discuss this in §10. Our code only uses the basic operations plus, minus, times, divide, and sqrt, and these operations are performed in such a way as to avoid arithmetic errors (such as taking the square root of a negative number.) It takes about 6 hours for our program to eliminate all configurations that are not within 2^{-14} , in the L^∞ norm, of a suitably normalized version of the TBP. See Lemma 2.3. Without the interval arithmetic, the code runs in about an hour.

Theorem 5.1 is the rate-determining step in our calculations. Numerical experimentation suggests that our bound in Theorem 5.1 is off by a factor somewhere between 2 and 4. In light of this fact, our calculation probably ought to be about 10 times faster than it is. We can certainly improve Theorem 5.1, but we haven't been able to think of a simple or dramatic improvement.

A nice feature of our program is that we have embedded it in a graphical user interface. The reader can watch the program in action and see how it samples the configuration space. The reader can also manually construct a rectangular solid subset of the configuration and then see a printout of all the computational tests that are applied to it. This graphical aspect doesn't add anything to the formal proof, but it makes it less likely we have made a gross computing error. We have tried to isolate the relatively small amount of computer code that goes into the actual proof, so that it can be more easily inspected.

The entire Java program is available from my website. See <http://www.math.brown.edu/~res/Electron/index.html>. The code is fairly well documented, and we're still working to improve the documentation. Aside from graphical support files, all the files involved in the proof have the **Interval** prefix. The directory contains a number of other files, which support other features of the program. Even though the proof portion of the code is done and working, the whole program is still somewhat in flux. I plan to gradually improve the code as time passes, and update it as I go.

1.5 Acknowledgements

I would like to thank Henry Cohn for helpful conversations about placing electrons on a sphere. Henry's great colloquium talk at Brown university this fall inspired me to work on this problem. I would also like to thank Jeff Hoffstein and Jill Pipher for their interest and encouragement while I worked on this problem. I would like to thank John Hughes for a very interesting discussion about interval arithmetic. Finally, I would like to say that I learned how to do interval arithmetic in Java by reading the source files from Tim Hickey's implementation, <http://interval.sourceforge.net/interval/index.html>.

2 Proof in Broad Strokes

2.1 Stereographic Projection

We find it convenient to work mainly with $\mathbf{C} \cup \infty$ rather than on S^2 . Our reason for this is that a configuration space based on points in \mathbf{C} has a natural flat structure, and lends itself well to a nice subdivision scheme. The subdivision scheme, which essentially amounts to cutting rectangular solids into smaller rectangular solids, feeds into our divide-and-conquer algorithm. All this is discussed in §2.5 below.

We map S^2 to $\mathbf{C} \cup \infty$ using *stereographic projection*:

$$\Sigma(x, y, z) = \frac{x}{1-z} + i \frac{y}{1-z}. \quad (3)$$

Σ is a conformal diffeomorphism which maps circles on S^2 to generalized circles in $\mathbf{C} \cup \infty$. A *generalized circle* is either a circle or a straight line. We have

$$\Sigma(0, 0, 1) = \infty. \quad (4)$$

Thus, Σ maps a circle $C \subset S^2$ to a straight line if and only if $(0, 0, 1) \in C$.

The inverse map is given by

$$\Sigma^{-1}(x + iy) = \left(\frac{2x}{1+x^2+y^2}, \frac{2y}{1+x^2+y^2}, 1 - \frac{2}{1+x^2+y^2} \right). \quad (5)$$

Let $\|\cdot\|$ denote the usual norm on \mathbf{R}^3 . Here are two pieces of metric information we will use later on:

$$\|\Sigma^{-1}(z) - \Sigma^{-1}(\infty)\| = \frac{2}{\sqrt{1+|z|^2}} \quad (6)$$

$$\left\| \frac{d\Sigma^{-1}}{dx} \right\| = \left\| \frac{d\Sigma^{-1}}{dy} \right\| = \frac{2}{1+x^2+y^2}. \quad (7)$$

Equations 6 and 7 both have straightforward derivations, which we omit. Slightly abusing notation, we define

$$E(z_1, z_2) = E(\Sigma^{-1}(z_1), \Sigma^{-1}(z_2)) \quad (8)$$

Here E can be any energy potential. for points $z_1, z_2 \in \mathbf{C} \cup \infty$. In this way, we can talk about the energy of a configuration of points in $\mathbf{C} \cup \infty$.

2.2 The Triangular Bi-Pyramid

As in the introduction $\|\cdot\|$ denotes the usual norm on \mathbf{R}^3 . Unless stated otherwise, all the distances we measure in \mathbf{R}^3 are taken with respect to the Euclidean metric. What we say here works for any energy potential.

In the TBP, we have the following information.

- One pair of points is 2 units apart.
- 3 pairs of points are $\sqrt{3}$ units apart.
- 6 pairs of points are $\sqrt{2}$ units apart.

Accordingly, the energy of the TBP, with respect to E , is

$$M_E = E(1/2) + 3E(\sqrt{3}) + 6E(\sqrt{2}). \quad (9)$$

It is well known that the regular tetrahedron minimizes the energy for 4 points. All points are $\sqrt{8/3}$ units apart. For this reason, the regular tetrahedron has energy

$$T_E = 6E(\sqrt{8/3}). \quad (10)$$

We can use this fact to get some crude bounds on 5-point configurations. Given a 5 point configuration P and a point $p \in P$, we define

$$E(P, p) = \sum_{q \in P \setminus \{p\}} E(\|p - q\|). \quad (11)$$

We have the immediate estimate

$$E(P) \geq E(P, p) + T_E. \quad (12)$$

Thus, if P is an energy minimizer we must have

$$E(P, p) \leq M_E - T_E; \quad \forall p \in P. \quad (13)$$

This is one of the criteria we will use to eliminate certain configurations from consideration.

We can also use Equation 13 to give information about pairs of points within a minimizing configuration. We will consider this in the next section.

2.3 Estimates for the Power Laws

The fairly weak results in this section are designed to give us some control on the size of the configuration space we must consider. For any given exponent, these results are just short calculations. It is only our desire to handle all exponents at the same time that adds complexity to the proof.

Lemma 2.1 *Let p, q_1, q_2 be 3 points of an energy minimizer with respect to a power law potential. Then $\|p - q_1\| > 1/2$.*

Proof: Let $E(r) = 1/r^e$. Since E is decreasing, $E(\|p - r\|) \geq E(2)$ for all $p, r \in S^2$, because S^2 has chordal diameter 2. In light of Equation 12, this lemma is true provided that

$$T_E + 3E(2) + E(1/2) - M_E > 0 \quad (14)$$

When E is as above, our problem boils down to showing that

$$\phi(e) = 2^{1-e} - 3^{1-e/2} + 2^e - 3^{1-e/2} + 2^{1-(3e)/2} 3^{1+e/2} > 0. \quad (15)$$

This is an exercise in calculus. We compute

$$\phi(0) = 0; \quad \phi'(0) > 0; \quad \phi''(0) > 1. \quad (16)$$

We compute $\phi'''(e) = A(e) - B(e)$, where

$$\begin{aligned} A(e) &= 3 \log(2)^2 2^{-2-e/2} + 2^e \log(2)^3 + \frac{\log(3)}{8} 3^{1-e/2} > 0; \\ B(e) &= 2^{1-e} \log(2)^3 + 2^{-2-(3e)/2} 3^{1+e/2} \log(8/3)^3 < 2. \end{aligned} \quad (17)$$

In short, $\phi'''(e) > -2$. Taylor's theorem with remainder now tells us that

$$\phi(e) > \frac{e^2}{2} - \frac{e^3}{3}. \quad (18)$$

Hence $\phi(e) > 0$ for $e \in (0, 3/2)$. A similar computation for ϕ' shows that

$$\phi'(e) > -10. \quad (19)$$

We compute that

$$\phi(3/2 + j/10) > 1; \quad j = 0, \dots, 85. \quad (20)$$

Combining the last two equations, we see that $\phi(e) > 0$ for all $e \in [3/2, 10]$. Finally, for $e > 10$, the result is obvious. ♠

Lemma 2.2 *Let p, q_1, q_2 be 3 points of an energy minimizer with respect to a power law potential. Assume that $E(\|p - q_2\|) \leq E(\|p - q_1\|)$. Then $\|p - q_1\| > 1/2$ and $\|p - q_2\| > 1$.*

Proof: We have the inequality

$$E(\|p - q_1\|) + E(\|p - q_2\|) \leq M_E - T_E - 2E(2). \quad (21)$$

Hence

$$E(\|p - q_2\|) \leq \frac{M_E - T_E - 2E(2)}{2}. \quad (22)$$

Establishing this inequality boils down to showing that

$$\phi(e) = 2 + 2^{1-e} - (3)(2^{1-e/2}) - 2^{-e} - 3^{1-e/2} + 2^{1-(3e)/2}3^{1+e/2} > 0. \quad (23)$$

This time we compute

$$\phi(0) = 0; \quad \phi'(0) > 0; \quad \phi''(0) > 1/4. \quad (24)$$

Examining the terms of ϕ''' , as in the previous lemma, we find that

$$\phi'''(e) > -12. \quad (25)$$

Taylor's theorem now tells us that $\phi > 0$ on $[0, 1/16)$. A similar computation shows

$$\phi'(e) > -10. \quad (26)$$

We now compute that

$$\phi(1/16 + j/2000) > 1/200; \quad j = 0, \dots, 1875. \quad (27)$$

Combining the last two equations, we see that $\phi(e) > 0$ for $e \in [1/16, 1]$. Next, we compute that

$$\phi(1 + j/100) > 1/10; \quad j = 0, \dots, 900. \quad (28)$$

This shows that $\phi(e) > 0$ for $e \in [1, 10]$. For $e > 10$ the result is again obvious.

2.4 Planar Configurations

We took the trouble to prove Lemmas 2.1 and 2.2 for any power law so that what we say in this section works for any power law.

Basic Definition: Let $P = \{p_0, \dots, p_4\}$ be a configuration of 5 points on S^2 . $Z = \Sigma(P) = \{z_0, \dots, z_4\}$ be the corresponding configuration in $\mathbf{C} \cup \infty$. We rotate S^2 so that

$$z_4 = \infty; \quad z_0 \in \mathbf{R}_+ \quad E(z_0, z_4) = \max_{i < j} E(z_i, z_j). \quad (29)$$

The TBP: Now we discuss what the TBP looks like with this normalization. The TBP has two kinds of points. We say that the *polar points* are the two antipodal points in the configuration. We say that the three remaining points are *equatorial*. When z_4 corresponds to a polar point, we have the following configuration, which is unique up to the permutation of z_1, z_2, z_3 :

$$z_0 = 1; \quad z_1 = \exp(-2\pi i/3); \quad z_2 = 0; \quad z_3 = \exp(2\pi i/3); \quad (30)$$

When z_4 corresponds to an equatorial point, we have

$$z_0 = 1; \quad z_1 = -i\sqrt{3}/2; \quad z_2 = -1 \quad z_3 = i\sqrt{3}/2; \quad (31)$$

Later on, we will use a symmetry argument to avoid having to deal with the second of these configurations.

The Space of Minimizers: We check 3 facts using Equation 6.

1. If $|z| = 1$ then $\|\Sigma^{-1}(z) - \Sigma^{-1}(\infty)\| = \sqrt{2}$.
2. If $|z| \geq 2$ then $\|\Sigma^{-1}(z) - \Sigma^{-1}(\infty)\| < 1$.
3. If $|x| \geq 4$ then $\|\Sigma^{-1}(z) - \Sigma^{-1}(\infty)\| < 1/2$.

Suppose now that Z is a minimizer for some power law potential. It follows from Lemma 2.1 and Item 3 that $|z_j| < 3$ for $j = 1, 2, 3$. It follows from Item 1 and Lemma 4.2 that $|z_0| \geq 1$. We conclude that $z_0 \in [1, 4]$. It follows Lemma 2.2 and Item 2 that $|z_j| \leq 2$ for $j = 1, 2, 3$. We conclude that all the configurations we need to consider lie in the compact region compact region $\Omega = [0, 4] \times [-2, 2]^6 \subset \mathbf{R}^7$. The map is given by just stringing out the

coordinates of the points z_0, z_1, z_2, z_3 .

Dyadic Objects: Given squares $Q_1, Q_2 \subset \mathbf{C}$, we write $Q_1 \rightarrow Q_2$ if Q_2 is one of the 4 squares obtained by dividing Q_1 in half along both directions. We say that a square Q is a *dyadic square* if there is a finite

$$[-2, 2]^2 \rightarrow Q_1 \rightarrow \dots \rightarrow Q_n = Q. \quad (32)$$

The sides of Q are necessarily parallel to the coordinate axes, and the vertices have dyadic rational coordinates. We call the dyadic square *normal* if it does not cross the coordinate axes. A single subdivision of $[-2, 2]$ produces normal dyadic squares.

We make the same definition for line segments as for squares., except that the notation $S_1 \rightarrow S_2$ means that S_2 is one of the two segments obtained by cutting S_1 in half. We say that a *dyadic segment* is a line segment S such that there is a finite chain

$$[0, 4] \rightarrow S_1 \rightarrow \dots \rightarrow S_n = S. \quad (33)$$

We say that a *dyadic box* in Ω is a set of the form $Q_0 \times Q_1 \times Q_2 \times Q_3$, where Q_0 is a dyadic segment and Q_j is a dyadic square for $j = 1, 2, 3$. The whole space Ω itself is a dyadic box.

Subdivision: Let $B_j = Q_{j0} \times Q_{j1} \times Q_{j2} \times Q_{j3}$ be a dyadic box for $j = 1, 2$. We write $B_1 \rightarrow_k B_2$ if

- $Q_{1i} = Q_{2i}$ for $i \neq k$.
- $Q_{1k} \rightarrow Q_{2k}$.

The *kth subdivision* of B_1 is the union of all B_2 such that $B_1 \rightarrow_k B_2$. When $k = 0$, this union consists of two dyadic boxes. When $k = 1, 2, 3$, the union consists of 4 dyadic boxes. The set of all dyadic boxes in Ω forms a directed tree. Each dyadic box points to $14 = 2 + 4 + 4 + 4$ smaller dyadic boxes.

The divide-and-conquer algorithm will be a depth-first search through this tree. It seems that the speed of the program depends a lot on how we do the subdivisions, so we will explain this in detail in the next section.

2.5 The Divide and Conquer Algorithm

Our discussion applies to a general power law potential, but we only apply the algorithm to the Coulomb potential.

Let $\epsilon > 0$ be some small number. In this section, we explain in the abstract how we show, with a finite calculation, that any winning configuration lies within ϵ of one of the two TBP configurations described in §2.4. There are 5 components to our program:

Confinement: We say that a dyadic box

$$\mathcal{Q} = Q_0 \times Q_1 \times Q_2 \times Q_3. \quad (34)$$

is ϵ -confining if, for each $j = 0, 1, 2, 3$, the dyadic square B_j is contained in the open square of side length ϵ centered on the point z_j from Equation 30.

Tetrahedral Eliminator: We eliminate \mathcal{Q} if it satisfies the hypotheses of Lemma 3.6. In this situation, every configuration in \mathcal{Q} violates Equation 13. This function speeds up our calculations quite a bit.

Redundancy Eliminator: We will isolate a subset $\Omega' \subset \Omega$ with the following property: If $Z \in \Omega - \Omega'$, then there is some $Z' \subset \Omega'$ (obtained by permuting the points of applying some obviously energy-decreasing move) such that $E(Z') \leq E(Z)$. In §4.4 we will describe some simple tests we use to show that $\mathcal{Q} \in \Omega - \Omega'$. We eliminate \mathcal{Q} if it passes one of these tests.

One convenient property of Ω' is that it contains the configuration in Equation 30 but not the configuration in Equation 31. This means that we can automatically eliminate configurations near the one in Equation 31. This is why our notion of ϵ -confinement only mentions the configuration in Equation 30.

Energy Estimator: Now we come to the main point. Say that an *energy estimator* is a function $\Phi : \mathcal{S} \rightarrow \mathbf{R}$ such with the following property. For every configuration $Z = \{z_0, \dots, z_4\}$ with $z_j \in Q_j$, we have

$$E(Z) \geq \Phi(\mathcal{Q}).$$

See Theorem 5.1 for the definition of our Energy Estimator. Theorem 5.1 is our main technical result.

Depth First Search: Recall that M_ϵ is the energy of the TBP. Our program maintains a list \mathcal{L} of dyadic boxes. Initially, \mathcal{L} just has the single box Ω , the whole space. At a given stage of the program, the algorithm examines the last box \mathcal{Q} and eliminates it if one of three things happens:

1. \mathcal{Q} is ϵ -confined.
2. Lemma 3.6 eliminates \mathcal{Q} .
3. One of the tests in §4.4 eliminates \mathcal{Q} .
4. $\Psi(\mathcal{Q}) > M_\epsilon$.

Otherwise, \mathcal{Q} is eliminated and to \mathcal{L} we append the dyadic boxes in the k th subdivision of \mathcal{Q} for some $k \in \{0, 1, 2, 3\}$. We will explain how k is determined momentarily. The algorithm halts if \mathcal{L} is the empty list. In this case, we have shown that, up to symmetries, any minimizer lies within ϵ of the TBP.

Subdivision Rule: The error term in Theorem 5.1 has the form

$$\sum_{i=0}^3 \sum_{j \neq i} \epsilon(Q_i, Q_j). \quad (35)$$

Here $\epsilon(Q_i, Q_j)$ is a quantity that depends on the geometry of Q_i and Q_j . Roughly, it varies quadratically with the side length of Q_i . We write

$$\epsilon(i) = \sum_{j \neq i} \epsilon(i, j). \quad (36)$$

Then, again, $\epsilon(i)$ depends roughly quadratically on the side length of Q_i . We find the index k that maximizes the function $i \rightarrow \epsilon(i)$ and then we use the k th subdivision rule. Thus, we subdivide in such a way as to try to make the error estimate in Theorem 5.1 as small as possible. When we compare this method with a more straightforward method of subdividing so as to keep the squares all about the same size, our method leads to a vastly faster computation.

Remark: The main difficulty in our proof is choosing an energy estimator that leads to a feasible calculation. We found the subtle Energy Estimator from Theorem 5.1 after quite a bit of trial and error.

2.6 The Main Results

Let \mathcal{E} denote the energy function on Ω . For any $s > 0$ let Ω_s denote those configurations $\{z_k\}$ so that z_k is contained in a square of side length s centered at the k th point of the TBP, normalized as in Equation 30. We shall be interested in the cases when

$$s = 2^{-11}. \tag{37}$$

Running our computer program, we prove the following result.

Lemma 2.3 (Confinement) *Any Coulomb energy minimizer in Ω has the same energy as some configuration in $\Omega_{s/4}$.*

Let H_e denote the Hessian of \mathcal{E} , with respect to the potential $E(r) = r^{-e}$. In §9 we will prove the following result.

Lemma 2.4 *For $e = 1, 2$ and for any $W \in \Omega_s$, the matrix $H_e(W)$ is positive definite.*

Now let Z_1 be a 5-point minimizer for the Coulomb potential. By the Confinement Lemma, we can find a new configuration $Z_2 \in \Omega_s$ with the same energy. But \mathcal{E} has positive definite Hessian throughout Ω_s , and (by symmetry) the gradient $\nabla\mathcal{E}$ vanishes at Z_0 , the TBP. Restricting \mathcal{E} to a straight line segment connecting Z_0 to Z_2 we see that \mathcal{E} is a convex function with a local minimum at Z_0 . Hence $\mathcal{E}(Z_2) > \mathcal{E}(Z_0)$. This proves Theorem 1.1.

Remarks:

- (i) Our program also establishes the Confinement Lemma for the function $E(r) = r^{-2}$. The same argument as above now establishes Theorem 1.2.
- (ii) We didn't need to compute all the way down to $\Omega_{s/4}$. We could have stopped at Ω_s in the Confinement Lemma. However, an earlier version of this paper had a weaker result on the Hessian, and we did the extra computing to accomodate this. There doesn't seem to be any reason to throw out our stronger computational result since we (or, rather, the computer) took the trouble to get it.

3 Separation Estimates

3.1 Overview

Let Σ be stereographic projection. The sets of interest to us have the form

$$Q^* = \Sigma^{-1}(Q). \tag{38}$$

where Q is either a dyadic segment or a dyadic square or the point ∞ . We will call Q a *dyadic planar set* and Q^* a *dyadic spherical patch*. A dyadic spherical patch is either the point $(0, 0, 1)$, or an arc of a great circle, or else a subset of the sphere bounded by 4 arcs of circles.

Let (Q_1, Q_2) where Q_j is a dyadic planar set. In this chapter we are interested in the following two quantities.

$$\psi_{\max}(Q_1, Q_2) = \max \|p_1 - p_2\|; \quad p_j \in Q_j^*. \tag{39}$$

$$\psi_{\min}(Q_1, Q_2) = \min \|p_1 - p_2\|; \quad p_j \in \text{Hull}(Q_j^*). \tag{40}$$

Here $\text{Hull}(Q_j^*)$ is the convex hull of Q_j^* . For technical reasons the lower bound we seek need to work for a slightly larger range of points.

In this chapter, we will estimate $\psi(Q_1, Q_2)$ in terms of quantities that can be determined by a finite computation. At the end of the chapter, we will give, as an application of these estimates, the definition of the Tetrahedral Eliminator discussed in §2.5.

In the next definitions, we set $z = x + iy$. If Q is a dyadic square or dyadic segment, we define

$$\begin{aligned} \underline{x} &= \min_{z \in Q} |x|; & \bar{x} &= \max_{z \in Q} |x|; & \underline{y} &= \min_{z \in Q} |y|; & \bar{y} &= \max_{z \in Q} |y|; \\ \delta &= \frac{2(\bar{x} - \underline{x})}{1 + \underline{x}^2 + \underline{y}^2}; & \tau &= \sqrt{\dim(Q)}. \end{aligned} \tag{41}$$

These quantities depend on Q but we usually suppress them from our notation. Here $\bar{x} - \underline{x}$ is just the sidelength of Q . The quantity δ is an estimate on the side length of Q^* . Note that $\tau = 1$ if Q is a dyadic segment and $\tau = \sqrt{2}$ if Q is a dyadic square.

When $Q = \{\infty\}$ we set $\delta = \tau = 0$ and we don't define the other quantities know Q^* exactly in this case.

Given a pair (Q_1, Q_2) of dyadic objects, we

$$D = \|\Sigma^{-1}(z_1) - \Sigma^{-1}(z_2)\|; \quad \delta = \frac{\delta_1\tau_1 + \delta_2\tau_2}{4}. \quad (42)$$

Here z_j is the center of Q_j and $\delta_j = \delta(Q_j)$, as defined above. Here is our main result.

Lemma 3.1 (Bound) *The following is true relative to any pair of dyadic patches.*

$$\psi_{\min} \geq D(1 - \delta^2/2) - (\sqrt{4 - D^2})\delta; \quad \psi_{\max} \leq D + (\sqrt{4 - D^2})\delta.$$

Remark: Our proof will yield the better bounds

$$\psi_{\min} \geq D \cos(\delta) - (\sqrt{4 - D^2}) \sin(\delta) \quad \psi_{\max} \leq D \cos(\delta) + (\sqrt{4 - D^2}) \sin(\delta),$$

but for computational reasons we want to avoid the trig functions. We have used rational replacements which are quite close in practice to the trig functions.

There is one situation where we can get a completely sharp upper bound. We define

$$\psi'_{\max}(Q_1, Q_2) = \max \|p_1 - p_2\|; \quad p_j \in Q_j^*. \quad (43)$$

This time we maximize over pairs (p_1, p_2) , where p_j is a vertex of Q_j^* . A finite computation gives ψ'_{\max} . We define ψ'_{\min} similarly. Recall that a dyadic square is normal if it doesn't cross the coordinate axes.

Lemma 3.2 (Perfect Bound) *If Q_1 is normal and $Q_2 = \{\infty\}$ then we have $\psi_{\max} = \psi'_{\max}$ and $\psi_{\min} = \psi'_{\min}$.*

We define Ψ_{\min} to be the best bound we can get from the two lemmas above (or 0, if no lemma applies.) We define Ψ_{\max} to be the best bound we can get from the two lemmas above (or 2, if no lemma applies.)

The rest of the chapter is devoted to proving Lemma 3.1 and Lemma 3.2.

3.2 Proof of Lemma 3.1

Lemma 3.3 *Let A and B be arcs of the unit circle. Let Δ_A and Δ_B denote the arc lengths of A and B . Let D_A and D_B denote the distance between the endpoints of A and B respectively. Let*

$$\delta = \frac{\Delta_A - \Delta_B}{2}.$$

Then

$$D_B = D_A \cos(\delta) \pm \left(\sqrt{4 - D_A^2} \right) \sin(\delta).$$

Proof: We have the relations

$$D_A = 2 \sin(\Delta_A/2); \quad D_B = 2 \sin(\Delta_B/2) = 2 \sin(\Delta_A/2 - \delta). \quad (44)$$

Hence, by the angle addition formula,

$$D_B = D_A \cos(\delta) - 2 \cos(\sin^{-1}(D_A/2)) \sin(\delta). \quad (45)$$

Noting that

$$\cos(\sin^{-1}(x)) = \sqrt{1 - x^2}, \quad (46)$$

we see that Equation 45 is the same as the result we want. ♠

Lemma 3.4 *Let Q be a dyadic set. Every point of Q^* is within $\delta\tau/2$ units of $\Sigma^{-1}(z_Q)$.*

Proof: When evaluated at all points of Q , the quantity in Equation 7 is maximized at the point $(\underline{x}, \underline{y})$. Its value at that point is exactly

$$\frac{2}{1 + \underline{x}^2 + \underline{y}^2} = \frac{\delta}{s}.$$

Therefore Σ^{-1} expands distances on Q by at most a factor of δ/s , and every point of Q is within $s\tau/2$ of z . From here the result is obvious. ♠

Now we give the main argument for Lemma 3.1. We consider the lower bound first. Given a point $p \in S^2$ and some $r > 0$ we let $H(p, \epsilon) \subset S^2$ denote

the convex hull of the set of points on S^2 that are within ϵ of p in terms of arc length on S^2 . We call such a set a *cap*.

It follows from Lemma 3.4 and the convexity of caps that

$$\text{Hull}(Q_j^*) \subset H_j = H(p_j, \delta_j \tau_j / 2). \quad (47)$$

Here $p_j = \Sigma^{-1}(z_j)$, where z_j is the center of Q_j .

Suppose first that H_1 and H_2 are disjoint. Let $(q_1, q_2) \in H_1 \times H_2$ be two points which realize the minimum of $\|q_1 - q_2\|$. We must have $q_j \in \partial H_j$. Also, the segment joining q_1 to q_2 must be perpendicular to both ∂H_1 and ∂H_2 . This situation leads to the result that q_1 and q_2 are contained on the great circle C joining p_1 and p_2 .

We can now reduce everything to a problem in the plane. Let Π be the plane containing C . We identify Π with \mathbf{C} , so that C is the unit circle. Figure 3.1 shows the situation. We have drawn the case when both intersections lie in a half-disk, but this feature is not a necessary part of the proof.

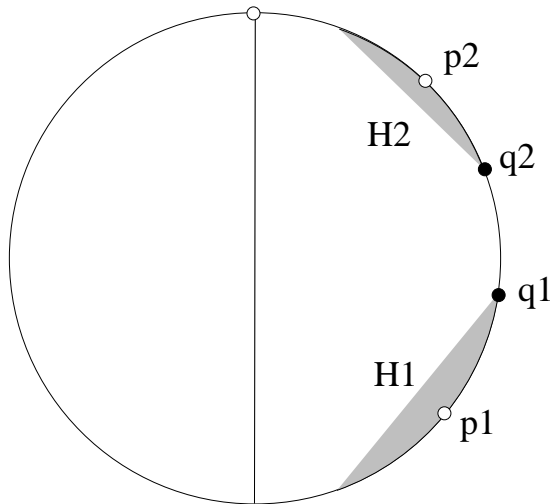


Figure 3.1: Two circular caps.

Let A be the short circular arc joining p_1 and p_2 , and let B be the short circular arc joining q_1 and q_2 . Referring to Lemma 3.3, we have

$$D_A = D(Q_1, Q_2) = \|p_1 - p_2\|; \quad (48)$$

Here $D = D(Q_1, Q_2)$ is the quantity in the statement of the lemma. We also have

$$\psi_{\min} \leq D_B = \|q_1 - q_2\|. \quad (49)$$

Finally, the length of the circular arc joining p_j to q_j is $\delta_j \tau_j / 2$. Therefore

$$\delta(A, B) = \Delta_A - \Delta_B = \frac{\delta_1 \tau_1 / 2 + \delta_2 \tau_2 / 2}{2} = \delta(Q_1, Q_2). \quad (50)$$

Applying Lemma 3.3, and using our three equations, we get

$$\psi_{\min} \geq D \cos(\delta) - \left(\sqrt{4 - D^2} \right) \sin(\delta) \quad (51)$$

But $\cos(\delta) \geq 1 - \delta^2$ and $\sin(\delta) \leq \delta$. This gives us the lower bound from Lemma 3.1 in the case the caps are disjoint.

When the caps intersect, we have $\psi_{\min} = 0$. We just want to show that the lower bound in Lemma 3.1 is nonpositive. We want to reduce this case to the previous one. Choose some small $\epsilon > 0$ and consider smaller caps H'_1 and H'_2 that are separated by a distance of exactly ϵ . These two caps are based on some number $\delta' < \delta$. Our argument in the previous case gives

$$\epsilon > D(1 - (\delta')^2/2) - \left(\sqrt{4 - D^2} \right) \delta' \quad (52)$$

$$D(1 - (\delta')^2/2) - \left(\sqrt{4 - D^2} \right) \delta' > D(1 - \delta^2/2) - \left(\sqrt{4 - D^2} \right) \delta. \quad (53)$$

Combining these two results, we see that the lower bound in Lemma 3.1 is less than ϵ . But ϵ is arbitrary. Hence, the lower bound in Lemma 3.1 is nonpositive in this case. This completes the proof of the lower bound.

The proof of the upper bound is similar. Suppose first that $H_1 \cap H_2$ does not contain a pair of antipodal points. Then, by Lagrange Multipliers, the pair of points (q_1, q_2) realizing the maximum lie on the great circle through p_1 and q_2 . We then rotate as above and apply the same argument. This time we get

$$\psi_{\max} \leq D \cos(\delta) + \left(\sqrt{4 - D^2} \right) \sin(\delta) \quad (54)$$

But $\cos(\delta) \leq 1$ and $\sin(\delta) \leq \delta$. This gives us the lower bound from Lemma 3.1 in the case $H_1 \cup H_2$ does not contain a pair of antipodal points.

If $H_1 \cup H_2$ contains a pair of antipodal points then one of two things is true. If p_1 and p_2 are antipodal points, then obviously the upper bound in Lemma 3.1 gives a number greater than 2. If p_1 and p_2 are not antipodal we can use the same shrinking trick that we used in the previous case to show that the upper bound in Lemma 3.1 gives a number that is at least 2. In either case, the upper bound still holds.

This completes the proof of Lemma 3.1.

3.3 Proof of Lemma 3.2

Lemma 3.5 *Suppose that Q_1 is a dyadic segment or square and $Q_2 = \{\infty\}$. Let $p_2 = (0, 0, 1)$. Then, for point $p_1 \in Q_1^*$ we have $\psi'_{\min} \leq \|p_1 - p_2\| \leq \psi'_{\max}$. In particular, the upper bound in Lemma 3.2 is true.*

Proof: Consider the lower bound first. The point $z_1 \in Q_1$ which minimizes

$$\|\Sigma^{-1}(z_1) - \Sigma^{-1}(\infty)\| \tag{55}$$

is the point furthest from the origin. But, since disks are convex, the point of Q_1 farthest from the origin is a vertex.

Now for the upper bound. The point of Q_1 that maximizes Equation 55 is the one closest to the origin. If a vertex of Q_1 does not minimize the distance to the origin, then (by Lagrange multipliers) some ray through the origin intersects a side of Q_1 at a right angle. Since the sides of Q_1 are parallel to the coordinate axes, this can only happen if Q_1 crosses one of the coordinate axes. But Q_1 does not cross the coordinate axes. ♠

Lemma 3.5 immediately gives the upper bound. For the lower bound (which makes a different statement) we need to deal with all the points in the convex hull $H_1 = \text{hull}(Q_1^*)$. Any point $q \in H_1$ that minimizes $\|q - (0, 0, 1)\|$ must lie on ∂H_1 . We claim that ∂H_1 is the union of the following

- Q_1^* .
- The flat quadrilateral F that is the convex hull of the vertices of Q_1^* .
- The convex hulls $H(E_j)$ of the edges E_1, \dots, E_4 of Q_1^* .

Each of these sets is a subset of H_1 and we easily check, in each case, that every point in each set is a boundary point. Since the union of these sets is a topological sphere, it must account for the entire boundary.

Our lemma above takes care of the case when $q \in Q_1^*$. If q is an interior point of F , then the segment joining $(0, 0, 1)$ to q is perpendicular to F . But F is completely contained in a hemisphere that has $(0, 0, 1)$ on its boundary, so no such segment can exist.

Finally, suppose that $q \in H(E_j)$. Note that $H(E_j)$ is contained in a plane Π which also contains $(0, 0, 1)$. But, considering the distance minimization problem in Π , we see that q cannot be an interior point of $H(E_j)$. (The picture looks just like the one drawn in Figure 3.1.) But then either $q \in Q_1^*$ or $q \in F$, the two cases we have already handled. This completes the proof.

3.4 The Tetrahedral Eliminator

Let \mathcal{Q} be a dyadic box, as in the previous section. As in Equation 13, the quantity M_E is the energy of the TBP and the quantity T_E is the energy of the regular tetrahedron. Let Ψ_{\max} be the upper bound on the distance between Q_1^* and Q_1^* as in §3.1.

Lemma 3.6 (Tetrahedral Eliminator) *Let \mathcal{Q} be a dyadic box. Suppose that there is some index i such that*

$$\sum_{j \neq i} E(d_{ij}) > M_E - T_E; \quad d_{ij} = \Psi_{\max}(Q_i, Q_j). \quad (56)$$

Then no configuration in \mathcal{Q} is a minimizer for the E -energy.

Proof: By construction $\|p_i - p_j\| \leq d_{ij}$ for all $p_i \in Q_i^*$ and $p_j \in Q_j^*$. Therefore

$$E(P, p_i) > \sum_{j \neq i} E(d_{ij}) > M_E - T_E \quad (57)$$

for any configuration P corresponding to a point in \mathcal{Q} . But then every such configuration violates Equation 13 and cannot be a minimizer. ♠

3.5 Discussion

We can get a cheap Energy Estimator using the fact that

$$\mathcal{E}(Z) \geq \sum_{i < j} E(d_{ij}); \quad d_{ij} = \Psi_{\max}(Q_i, Q_j). \quad (58)$$

However, experiments lead us to believe that the main calculation would effectively take forever using this estimator.

Here is the problem: Even though $E(d_{ij})$ gives a good estimate for the minimum energy of a pair of points $(p_i, p_j) \in Q_i^* \times Q_j^*$, there is no guarantee that we can find a single configuration $\{p_j\}$ such that each d_{ij} is nearly realized by $E(\|p_i - p_j\|)$. So, the minimum energy of a configuration we can actually produce might be much higher than our estimate. That is, our estimate might not be that good *globally* (for all 10 interactions) even though it is good *locally* (for pairs of interactions.) We need to work harder to get a globally good energy estimator. This is the content of Theorem 5.1.

4 The Redundancy Eliminator

The constructions in this chapter work for any power law, and most of the constructions (just symmetry) work for any decreasing energy function.

4.1 Inversion

An *inversion* is a conformal involution ρ of $\mathbf{C} \cup \infty$ that fixes some circle C pointwise. We call ρ *stereo-isometric* if $\Sigma^{-1}(C)$ is a great circle of S^2 . This condition means that stereographic projection conjugates ρ to an isometry of S^2 . The purpose of this section is to prove the following lemma. The reader might want to just note the result and skip the proof on the first reading.

Lemma 4.1 *Let ρ be a stereo-isometric inversion fixing a circle centered on a point of $[1, \infty) \subset \mathbf{R}$. Let $X \subset \mathbf{C}$ be a strip bounded by horizontal lines, one lying above \mathbf{R} and one lying below \mathbf{R} . Let $X_- \subset X$ denote those points $z = x + iy$ with $x < 1 - \sqrt{2}$. Then $\rho(X_-) \subset \text{interior}(X) - X_-$.*

Proof: Being an inversion, the map ρ has 3 nice geometric properties.

- ρ interchanges the disk D bounded by C with its complement.
- ρ interchanges the center of C with ∞ .
- ρ preserves each ray through the center of C .

We will use these properties in our proof.

Let z_0 be the center of C . We claim that C separates z_0 from any point on \mathbf{R} that lies to the left of $1 - \sqrt{2}$. Let $p_0 = \Sigma^{-1}(z_0)$. As usual, $(0, 0, 1) = \Sigma^{-1}(\infty)$. Let Π be the plane equidistant between p_0 and $(0, 0, 1)$. Then

$$C = \Sigma(\Pi \cap S^2) \tag{59}$$

Let H be the half-space bounded by Π that contains p_0 .

The point p_0 lies on the great circle connecting $\Sigma^{-1}(1) = (1, 0, 0)$ to $(0, 0, 1)$. Since $z_0 \in [1, \infty)$, the point p_0 lies on the short arc connecting $(1, 0, 0)$ to $(0, 0, 1)$. But then

$$q = \Sigma^{-1}(1 - \sqrt{2}) = \left(-\frac{1}{\sqrt{2}}, 0, -\frac{1}{\sqrt{2}} \right) \notin \text{interior}(H). \tag{60}$$

The extreme case occurs when $p_0 = (1, 0, 0)$. In this extreme case $q \in \Pi \cap S^2$. As p_0 moves towards $(0, 0, 1)$, $H \cap S^2$ moves away from q . Since H does not contain $(0, 0, 1)$ either, the entire arc connecting q to $(0, 0, 1)$ is disjoint from the interior of H . But this means that C separates z_0 from all points of \mathbf{R} that lie to the left of $1 - \sqrt{2}$. This proves our claim.

Let D be the disk bounded by C that contains z_0 . From what we have already shown, the interior of D is disjoint from the vertical line L through $1 - \sqrt{2}$. Therefore $D \cap X_- = \emptyset$. Since ρ swaps D and its complement, we have

$$\rho(X_-) \subset D. \tag{61}$$

Hence

$$\rho(X_-) \cap X_- = \emptyset. \tag{62}$$

At the same time, ρ preserves all rays through the z_0 , the center of D . Noting again that $z_0 \in \mathbf{R}$, we see geometrically that $\rho(w)$ is closer to \mathbf{R} than w for all $w \in X - D$. See Figure 4.1. In particular, we have

$$\rho(X_-) \subset \text{interior}(X). \tag{63}$$

The first statement of the lemma now follows from Equations 62 and 63. The second statement follows from the first statement and from the fact that ρ is an involution. ♠

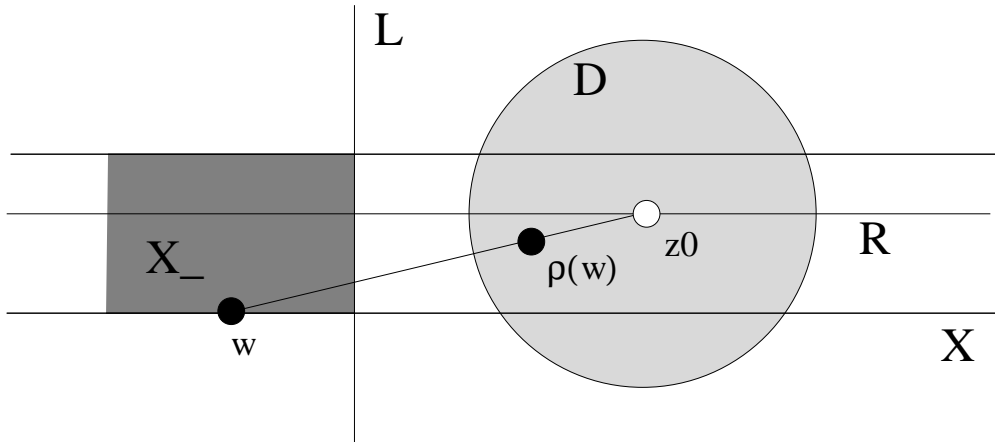


Figure 4.1: Inversion

4.2 A Lemma about Five Points

The result in this section is certainly well known. We suggest that perhaps the reader just note the result and skip the proof on the first reading.

Lemma 4.2 *Let P be any configuration of 5 distinct points on S^2 . Then some pair points of P are within $\sqrt{2}$ units of each other.*

Proof: A *quarter sphere* B is a region on S^2 bounded by two semicircular great arcs, meeting at antipodal points, such that the interior angles at the intersection points are $\pi/2$. The *axis* of B is the circular arc, contained in B , that connects the midpoints of the two bounding arcs. We will use the following easy-to-prove principle: If p is any point on the axis of B , then the closed hemisphere centered at p contains B . Call this *Property X*.

The lemma has a trivial proof if P contains two antipodal points, so we assume this is not the case. Let H_j be the closed hemisphere centered at p_j of P . Another way to state this lemma is that there are indices $i \neq j$ such that $p_i \in H_j$. Assume this is false, for the sake of contradiction.

Let N denote the hemisphere centered at $(0, 0, 1)$, and let S denote the opposite hemisphere. We normalize so that $p_0 = (0, 0, 1)$. By assumption, $p_1, \dots, p_4 \in S - N$. Since P does not contain antipodal points, P does not contain $(0, 0, -1)$. But then, for $j = 1, 2, 3, 4$, there is a unique point p_j^* on the equator $N \cap S$ which is as close as possible to p_j .

Let H_j^* denote the hemisphere centered centered at p_j^* . By construction, $H_j^* \cap S$ is a quarter sphere and p_j is a point on its axis. By Property X, we have $H_j^* \cap S \subset H_j$. But then, by assumption, $p_i \notin H_j^*$ if $i \neq j$. Let $\pi : S \rightarrow \mathbf{R}^2$ be the projection map $\pi(x, y, z) = (x, y)$. Then $\pi(S)$ is the unit disk and $\pi(S \cap H_j^*)$ is a half disk. Finally, $\pi(p_i)$ and $\pi(p_i^*)$ lie on the same ray through the origin. For this reason, $p_i \in H_j^*$ if and only if $p_i^* \in H_j^*$. Since $p_i \notin H_j^*$, we conclude that $p_i^* \notin H_j^*$.

Now we know that $p_i^* \notin H_j^*$ if $i \neq j$. Hence, the distance from p_i^* to p_j^* is greater than $\pi/2$. But then we have 4 points p_1^*, \dots, p_4^* , contained on the equator, each of which is more than $\pi/2$ from any of the other points. This is a contradiction. ♠

4.3 The Set of Good Configurations

Recall that Ω is our configuration space. Our construction here works for any energy function E . In this section we define the set $\Omega' \subset \Omega$, as discussed in §2.5 in connection with the Redundancy Eliminator.

Let $Z = \{z_0, \dots, z_4\}$ be a configuration of points in $\mathbf{C} \cup \infty$, normalized as in §2.4. We write $z_j = x_j + iy_j$. Also, we set $p_j = \Sigma^{-1}(z_j)$. Let Ω' be the set of configurations Z having all the following properties.

1. $\|p_i - p_j\| \leq \|p_0 - p_4\|$ for all indices $i \neq j$. Also $x_0 \geq 1$.
2. $y_1 \leq 0 \leq y_2 \leq y_3$.
3. If $y_1 < 0 < y_3$ then $x_2 \geq 1 - \sqrt{2}$.

Lemma 4.3 *For any $Z \in \Omega$, there exists $Z' \in \Omega'$ such that $E(Z') \leq E(Z)$.*

Proof: Permuting the points, we can the first half of Property 1. By Lemma 4.2 and the first half of Property 1, we must have $\|p_0, p_4\| \leq \sqrt{2}$. But this fails if $z_0 \in [0, 1)$. Hence $x_0 \geq 1$. In short, the first half of Property 1 implies the second half.

Reflecting in \mathbf{R} , we can arrange that $y_2 \geq 0$. Permuting again, we can retain Property 1 and arrange that $y_1 \leq y_2 \leq y_3$. To get Property 2, we just have to deal with the situation when $0 < y_1$. Let Z' be the new configuration obtained when we replace z_1 with the conjugate \bar{z}_1 and otherwise keep the points the same. Let P and P' be the corresponding configurations in S^2 . The points p_0, \dots, p_5 are all contained in the hemisphere bounded by the great circle

$$C = \Sigma^{-1}(\mathbf{R} \cup \infty). \quad (64)$$

The configuration P' is obtained from P simply by reflecting p_1 across C . But, as can be seen from e.g. the Pythagorean theorem, we then have $\|p'_1 - p_j\| \geq \|p_1 - p_j\|$ for $j \neq 3$. The other distances do not change. Since E is a monotone decreasing function, we have $E(Z') \leq E(Z)$. This gives us Property 2.

It remains to deal with Property 3. Suppose that $y_1 < 0 < y_3$ and $x_2 < 1 - \sqrt{2}$. Let ρ be the stereo-isometric inversion that swaps z_0 and z_4 . Let $Z' = \rho(Z)$. Let $z'_j = \rho(z_j)$. We set $z'_j = x'_j + iy'_j$. By construction Z' has property 1. By symmetry,

$$y'_1 < 0 < y'_3; \quad y'_2 \geq 0. \quad (65)$$

There are two cases to consider.

Case 1: Suppose first that

$$y'_2 \leq y'_3 \tag{66}$$

Equations 65 and 66 combine to say that Z' has Property 2 as well. Let X be the strip bounded by the horizontal lines through z_1 and z_3 . Then X satisfies the hypotheses of Lemma 4.1. Moreover, $z_2 \in X_-$, the half-strip from Lemma 4.1. Then $z'_2 \in X - X_-$ by Lemma 4.1. Hence $x'_2 > 1 - \sqrt{2}$. This shows that Z' has Property 3. Hence $Z' \in \Omega'$.

Case 2: Suppose that $y'_2 > y'_3$. Then we let Z'' be the configuration obtained from Z' by swapping z'_2 and z'_3 . Then Z'' satisfies Properties 1 and 2. The argument in Case 1 again shows that $z'_2 \in X - X_-$. In particular, $z'_2 \in X$. By construction,

$$z_3 \notin \text{interior}(X). \tag{67}$$

By Lemma 4.1, we have

$$\rho(X_-) \subset \text{interior}(X). \tag{68}$$

Combining these last two equations, we see that

$$z_3 \notin \rho(X). \tag{69}$$

Since ρ is an involution, this last equation gives us

$$z'_3 \notin X_-. \tag{70}$$

Summarizing the situation, we now know that

$$z'_2 \in X; \quad z'_3 \notin X_-. \tag{71}$$

Since $0 < y'_3 < y'_2$ and $z'_2 \in X$, we have

$$z'_3 \in X. \tag{72}$$

Combining the last two equations, we have

$$z'_3 \in X - X'; \quad \implies \quad x''_2 = x'_3 \geq 1 - \sqrt{2}. \tag{73}$$

The first statement implies the second. The second statement shows that Z'' has Property 3 as well. Finally, $E(Z'') = E(Z)$. ♠

4.4 The Main Construction

Now we define the Redundancy Eliminator discussed in §2.5. The redundancy eliminator performs 4 tests, one per property discussed above. Let $\mathcal{Q} = Q_0 \times Q_1 \times Q_2 \times Q_3$ be a dyadic box. As usual, a configuration $Z \in \mathcal{Q}$ defines points p_0, \dots, p_4 , with $p_j \in Q_j^*$.

Property 1: Let Ψ_{\max} and Ψ_{\min} be the separation functions from §3.1. We eliminate \mathcal{Q} if

$$\Psi_{\max}(Q_i, Q_j) < \Psi_{\min}(Q_0, Q_4) \quad (74)$$

for some pair of indices $i < j$ such that $(i, j) \neq (0, 4)$. We also eliminate \mathcal{Q} if $\underline{x}_0 < 1$.

Property 2: Let \underline{x}_j , etc be as in §3.1. We eliminate \mathcal{Q} if any of the following is true.

- $\underline{y}_1 \geq \bar{y}_2$;
- $\underline{y}_2 \geq \bar{y}_3$.
- $\bar{y}_2 \leq 0$.
- $\underline{y}_1 \geq 0$.

In the first 3 cases, the fact that we are using a weak inequality rather than a strict inequality means that sometimes we eliminate some configurations that lie in $\partial\Omega'$. Since we want to consider every configuration in Ω' , we need to justify this. We give the justification in the next section.

Property 3: We eliminate \mathcal{Q} if all of the following happen.

- $\bar{y}_1 < 0$.
- $\underline{y}_3 > 0$.
- $\bar{x}_2 < 1 - \sqrt{2}$.

This time there are no boundary cases to worry about.

4.5 Discussion of Boundary Cases

Here we discuss the use of weak inequalities in connection with Property 2 in the previous section. First of all, the reason why we want to do this is that it speeds up the computation. For example, were we to keep dyadic boxes with $\bar{y}_2 = 0$ we would need to consider many more dyadic boxes that are near the TBP.

The justification for why we can use weak inequalities is that all the configurations in $\partial\Omega'$ that we eliminate are actually counted twice, and we do not eliminate the relevant dyadic boxes both times.

To clarify the situation, we make the interpretation that our dyadic squares Q_2 and Q_3 are missing their top boundaries and Q_1 is missing its bottom boundary. With this convention, the divide and conquer algorithm from §2.5 examines every point in the configuration space except those for which $|y_j| = 2$ for some j . These configurations are not minimizers. See the discussion in §2.4. The main point here is that the union of “quarter-open” dyadic squares in the subdivision of a “quarter open” dyadic square is still equal to the original “quarter open” dyadic square. In the case of Q_2 and Q_3 , the bottom edges fill in for the top edges. In the case of Q_1 the top edges fill in for the bottom ones.

With this interpretation, we can simply eliminate the dyadic box \mathcal{Q} mentioned above, because it contains no configurations in Ω' . Adopting this convention has no effect whatsoever on our program. It is simply a question of how we interpret the output of the program.

5 The Energy Estimator

5.1 Preliminaries

We fix some value of n . Say that a *block* \mathcal{Q} is a collection Q_0, \dots, Q_n of dyadic objects, with $Q_n = \{\infty\}$ and all the other objects either segments or squares. Say that a collection of points z_0, \dots, z_n of points is *dominated by* the block if $z_k \in Q_k$ for all k . In our application, we will take $n = 4$. In this case, the set of configurations dominated by a block is precisely a dyadic box.

Remark: Though we always take Q_k to be a dyadic segment or square for $k = 0, \dots, n - 1$, the interested reader will note that everything we do works the same way with the milder constraint that each Q_k is either a segment in $[0, \infty)$ or a square with sides parallel to the coordinate axes that does not cross the coordinate axes.

We say that $\{z_k\}$ is a *vertex configuration* if z_k is a vertex of Q_k for $k = 0, \dots, n$. There is a finite list of vertex configurations. Given an energy function E , we define

$$\mathcal{E}(\mathcal{Q}) = \min_Z E(Z). \quad \mathcal{E}'(\mathcal{Q}) = \min_{Z'} E(Z'). \quad (75)$$

The first minimum is taken over all configurations Z dominated by \mathcal{Q} and the second minimum is taken over all vertex configurations Z' . The purpose of our main result in this chapter is to bound the quantity

$$\mathbf{ERR}(\mathcal{Q}) = \mathcal{E}'(\mathcal{Q}) - \mathcal{E}(\mathcal{Q}) \quad (76)$$

in terms of \mathcal{Q} .

We are interested mainly in the case when the function E is a power law, but we will state things more generally just to clarify the formulas we get. We suppose that E is convex decreasing and satisfies the following property. If $0 < r_2 \leq r_1$ then there are constants $c \geq 1$ and $h \geq 0$ (depending on everything) such that

$$\frac{E'(r_2)}{r_2} = c \frac{E'(r_1)}{r_1}; \quad E''(r_2) = (c + h)E''(r_1). \quad (77)$$

This condition could be stated more simply, but we have stated exactly the version we will use in Lemma 6.4, the one place where we use it. Other than this one place, the rest of our argument works for any convex decreasing function. The power law functions all satisfy these conditions with $h = 0$.

5.2 The Main Result

We defined Ψ_{\min} in §3.1. Given two dyadic objects Q and \widehat{Q} , we define

$$R = \Psi_{\min}(Q, \widehat{Q}). \quad (78)$$

When $R = 0$, our bound gives ∞ , a result that holds no matter what. So, without loss of generality, we treat the case when $R > 0$. In this case, the two sets Q^* and \widehat{Q}^* are contained in disjoint convex sets.

We define

$$\epsilon(Q, \widehat{Q}) = \max(0, \Lambda_1) + \Lambda_2. \quad (79)$$

When Q is a dyadic segment,

$$\Lambda_1 = \frac{R}{32}E'(R) + \left(\frac{1}{8} - \frac{R^2}{32}\right)E''(R); \quad \Lambda_2 = -\frac{E'(R)}{8} \quad (80)$$

When Q is a dyadic square,

$$\Lambda_1 = \frac{R}{16}E'(R) + \left(\frac{1}{4} - \frac{R^2}{16}\right)E''(R); \quad \Lambda_2 = -\frac{E'(R)}{7.98} \left(\sqrt{1 + \bar{x}^2} + \sqrt{1 + \bar{y}^2}\right). \quad (81)$$

Let δ_i be as in Equation 41, relative to Q_i . Recall that δ_i is a good estimate for the side length of the spherical patch Q_i^* . Also, let $\epsilon_{ij} = \epsilon(Q_i, Q_j)$.

Theorem 5.1 (Energy Estimator) *Let $\mathcal{Q} = (Q_0, \dots, Q_n)$ be any block. Then*

$$\mathbf{ERR}(\mathcal{Q}) \leq \sum_{i=0}^{n-1} \sum_{j \neq i} \epsilon_{ij} \delta_i^2.$$

Again, we remark that the case $n = 4$ is the case of interest to us. For reference, we work out the power-law case $E(r) = r^{-e}$ explicitly. When Q is a dyadic segment,

$$\Lambda_1 = \frac{e(e+1)}{8R^{e+2}} - \frac{e(e+2)}{32R^e}; \quad \Lambda_2 = \frac{e}{8R^{e+1}}. \quad (82)$$

When Q is a dyadic square,

$$\Lambda_1 = \frac{e(e+1)}{4R^{e+2}} - \frac{e(e+2)}{16R^e}; \quad \Lambda_2 = \frac{e}{7.98R^{e+1}} \left(\sqrt{1 + \bar{x}^2} + \sqrt{1 + \bar{y}^2}\right) \quad (83)$$

5.3 The Beginning of the Proof

Recall that a *partition of unity* is a collection of functions that sum to 1 at every point. A *point weighting* assigns a partition of unity

$$\lambda_{ab} : Q \rightarrow [0, 1]; \quad a, b \in \{0, 1\} \quad (84)$$

to each dyadic square Q and a partition of unity

$$\lambda_a : Q \rightarrow [0, 1]; \quad a \in \{0, 1\} \quad (85)$$

to each dyadic segment. We have a specific point weighting in mind, and we will define it in §8.

We let the vertices of a dyadic square Q be Q_{ab} for $a, b \in \{0, 1\}$. Here Q_{00} is the lower left vertex and the remaining vertices, traced in counterclockwise order, are Q_{10} , Q_{11} , Q_{01} . We let the vertices of a dyadic segment Q be Q_0 and Q_1 , with Q_0 on the left.

Given two points $z, w \in \mathbf{C} \cup \infty$, we define

$$f(z, w) = \frac{1}{\|\Sigma^{-1}(z) - \Sigma^{-1}(w)\|^e}. \quad (86)$$

Let \mathcal{X} denote the set of disjoint pairs (Q, \widehat{Q}) , as in the previous section. Let $\epsilon : \mathcal{X} \rightarrow \mathbf{R}$ be as in the previous section. We will spend the next 3 chapters proving the following result.

Lemma 5.2 *There exists a point weighting such that the following is true for all $(Q, \widehat{Q}) \in \mathcal{X}$.*

- *When Q is a segment*

$$\left(\sum_a \lambda_a(z) f(Q_a, w) \right) - f(z, w) < \epsilon(Q, \widehat{Q}) \delta(Q)^2; \quad \forall (z, w) \in Q \times \widehat{Q}.$$

- *When Q is a square*

$$\left(\sum_{a,b} \lambda_{ab}(z) f(Q_{ab}, w) \right) - f(z, w) < \epsilon(Q, \widehat{Q}) \delta(Q)^2; \quad \forall (z, w) \in Q \times \widehat{Q}.$$

Proof of Theorem 5.1: For ease of exposition, we will assume that the dyadic objects Q_0, \dots, Q_{n-1} are all dyadic squares. The case when there are some segments involved presents only notational complications. Consider a configuration z_0, \dots, z_n , dominated by \mathcal{Q} , that realizes $\mathcal{E}(\mathcal{Q})$. For each $i = 0, \dots, n$, define

$$B_i = \{z_0\} \times \{z_{i-1}\} \times Q_i \times \dots \times Q_n. \quad (87)$$

Just to be explicit, the two extreme cases are

$$B_0 = Q_0 \times \dots \times Q_n; \quad B_n = \{z_0\} \times \dots \times \{z_n\}. \quad (88)$$

(Recall that $Q_n = \{z_n\}$.) The set B_i is a $(2n - 2i)$ -dimensional rectangular solid. Let $\mathcal{E}_1(i)$ denote the minimum energy taken over all configurations of B_i . Let $\mathcal{E}_2(i)$ denote the minimum energy over all vertex configurations of B_i . The conclusion of this lemma is exactly

$$\mathcal{E}_2(0) - \mathcal{E}_1(0) \leq \sum_{i=0}^{n-1} \sum_{j \neq i} \epsilon_{ij} \delta(Q_i)^2 \quad (89)$$

We have $\mathcal{E}_2(n) = \mathcal{E}_1(n)$, because B_n is a single point. Hence, we have the telescoping sum

$$\mathcal{E}_2(0) - \mathcal{E}_1(0) = \sum_{i=0}^{n-1} \left(\mathcal{E}_2(i) - \mathcal{E}_1(i) \right) - \left(\mathcal{E}_2(i+1) - \mathcal{E}_1(i+1) \right) \quad (90)$$

Our choice of $\{z_i\}$ as a minimizing configuration implies that $\mathcal{E}_1(i)$ is independent of i . Combining this with Equation 90, we get

$$\mathcal{E}_2(0) - \mathcal{E}_1(0) = \sum_{i=0}^{n-1} \mathcal{E}_2(i) - \mathcal{E}_2(i+1). \quad (91)$$

To establish Equation 89, it suffices to prove

$$\mathcal{E}_2(i) - \mathcal{E}_2(i+1) \leq \sum_{j \neq i} \epsilon_{ij} \delta_i^2; \quad \forall i = 0, \dots, n-1. \quad (92)$$

For the remainder of the proof, we fix some $i \in \{0, \dots, n-1\}$ once and for all. We can find vertices v_{i+1}, \dots, v_n of Q_{i+1}, \dots, Q_n respectively such that

$$E(z_1, \dots, z_i, v_{i+1}, \dots, v_n) = \mathcal{E}_2(i+1). \quad (93)$$

Here $E(\dots)$ is the energy of the configuration. Note that Q_n is a singleton, so that our “choice” of v_n is forced.

For any choice of $a, b \in \{0, 1\}$, let Q_{iab} be the corresponding vertex of Q_i . Let

$$\lambda_{ab} = \lambda_{ab}(z_i) \tag{94}$$

be as guaranteed by Lemma 5.2. The function λ_{ab} depends on i , but we suppress this from our notation.

Since $\mathcal{E}_2(i)$ is the minimum energy of any vertex configuration of B_i ,

$$E(z_1, \dots, z_{i-1}, Q_{iab}, v_{i+1}, \dots, v_n) \geq \mathcal{E}_2(i). \tag{95}$$

Hence,

$$\mathcal{E}_2(i) - \mathcal{E}_2(i+1) \leq A_{ab};$$

$$A_{ab} = E(z_1, \dots, z_{i-1}, Q_{iab}, v_{i+1}, \dots, v_n) - E(z_1, \dots, z_i, v_{i+1}, \dots, v_n). \tag{96}$$

Setting $w_j = z_j$ for $j < i$ and $w_j = v_j$ for $j > i$, we have

$$\begin{aligned} \mathcal{E}_2(i) - \mathcal{E}_2(i+1) &\leq \\ &\sum_{a,b} \lambda_{ab} A_{ab} =^1 \\ &\sum_{a,b} \lambda_{ab} \left(\sum_{j \neq i} f(Q_{iab} w_j) - f(z_i, w_j) \right) =^2 \\ &\sum_{j \neq i} \sum_{a,b} \lambda_{ab} \left(f(Q_{iab}, w_j) - f(z_i, w_j) \right) =^3 \\ &\sum_{j \neq i} \left(\sum_{a,b} \lambda_{ab} f(Q_{iab}, w_j) \right) - f(z_i, w_j) \leq \\ &\sum_{j \neq i} \epsilon_{ij} \delta_i^2. \end{aligned} \tag{97}$$

The first inequality comes from Equation 96 and from the fact that $\sum \lambda_{ab} = 1$. Equality 1 comes from the cancellation of all terms not involving the i th index when we subtract the two sums for A_{ab} . Equality 2 comes from switching the order of summation. Equality 3 comes from the fact that $\sum_{ab} \lambda_{ab} = 1$. The last inequality follows from Lemma 5.2. This establishes Equation 92, which is all we need to prove Theorem 5.1. ♠

6 An Estimate for Line Segments

6.1 The Main Estimate

In this chapter we prove an estimate that relates directly to the Λ_1 term in our Energy Estimator. The reader might want to simply note the main result in this chapter on the first reading, and then come back to the proof later on. Let E be as in the previous chapter.

Let $p \in S^2$ be some point. In terms of Lemma 5.2, we think of p as being some point in the spherical patch $(\widehat{Q})^*$. Let $A' \subset \mathbf{R}^3 - \{p\}$ be a segment whose endpoints lie in S^2 . In terms of Lemma 5.2, we think of A' as joining two boundary points of the spherical patch Q^* . We define

$$F(q) = E(\|p - q\|) \tag{98}$$

Here F depends on p , but we suppress this from our notation.

Define

$$A'_x = (1 - x)A'_0 + xA'_1; \quad x \in [0, 1]. \tag{99}$$

Then $x \rightarrow A'_x$ is a constant speed parameterization of A' .

Lemma 6.1 (Segment Estimate) *Suppose that p is at least R units from every point of A' . Let δ be the length of A' .*

$$(1 - x)F(A'_0) + xF(A'_1) - F(A'_x) \leq \frac{X\delta^2}{8},$$

where

$$X = \frac{R}{4}E'(R) + \left(1 - \frac{R^2}{4}\right)E''(R).$$

Remark: We wish to point out one unfortunate feature of our notation. The quantities E' and E'' are derivatives of E whereas the quantity A' is simply a chord of S^2 . We make this notation because, in the next chapter, we will consider an arc A of S^2 and the chord A' that joins the endpoints of A . In some sense, the chord A' is a linear approximation to the arc A and the derivative E' is a linear approximation to the function E .

6.2 Strategy of the Proof

Lemma 6.1 really just involves the single variable function $\phi(x) = F(A'_x)$ defined for $x \in [0, 1]$. In §6.3 we prove the following easy estimate.

Lemma 6.2

$$(1-x)\phi(0) + x\phi(1) - \phi(x) \leq \frac{H}{8}; \quad H = \sup_{x \in [0,1]} \phi''(x).$$

Here $\phi''(x)$ is the second derivative with respect to x .

Recall that δ is the length of S . Let s denote the arc-length parameter along the segment S . We set things up so that $s = 0$ corresponds to S_0 and $s = \delta$ corresponds to S_1 . In general, the parameter $s \in S$ corresponds to $x = s/\delta \in [0, 1]$. In §6.5 we establish the following result.

Lemma 6.3 *Suppose we have the hypotheses in Lemma 6.1. Then,*

$$\frac{d^2\phi}{ds^2} \leq \frac{R}{4}E'(R) + \left(1 - \frac{R^2}{4}\right)E''(R).$$

By the Chain Rule, we have

$$\phi''(x) = \delta^2 \frac{d^2\phi}{ds^2}. \quad (100)$$

at corresponding points.

Lemma 6.1 follows from Lemma 6.2, Lemma 6.3, and Equation 100.

6.3 Proof of Lemma 6.2

We will prove Lemma 6.2 for a smooth function $h : [0, 1] \rightarrow \mathbf{R}$. We want to show that

$$(1-x)h(0) + xh(1) - h(x) \leq \frac{H}{8}; \quad H = \sup_{x \in [0,1]} h''(x). \quad (101)$$

Let c be any nonzero constant and let L be any linear function. Equation 101 holds for the function h if and only if it holds for ch . Likewise, Equation 101 holds for $h - L$ if and only if Equation 101 holds for h . Using these two

symmetries, it suffices to prove Equation 101 in the case when $h(0) = h(1) = 0$ and $H = 1$. In this case, Equation 101 simplifies to

$$-h(x) \leq \frac{1}{8}. \quad (102)$$

Let $a \in [0, 1]$ be a point where $-h$ attains its maximum. That is, h attains its minimum at a . Replacing h by the function $x \rightarrow h(1-x)$ if necessary, we can suppose without loss of generality $a \geq 1/2$.

We have $h'(a) = 0$ and, by the Fundamental Theorem of Calculus,

$$h'(x) = \int_a^b h''(t) dt \leq x - a \quad (103)$$

for all $x \in [a, 1]$. But then

$$-h(a) = h(1) - h(a) = \int_a^1 h'(x) dx \leq \int_a^1 x - a dx = \frac{(1-a)^2}{2} \leq \frac{1}{8} \quad (104)$$

This completes the proof. ♠

6.4 Comparison Lemmas

Let p and f be as above. Say that a *flag* is a pair (q, L) where L is a line and $q \in L$ is a point, and $q \neq p$. We define the following quantities.

- $r(q, L)$ is the distance from p to q .
- $d(q, L)$ is the distance from p to L .
- $\theta(q, L)$ is the small angle between \overline{pq} and L .
- $D(q, L) = F''(q)$, the second derivative w.r.t. arc length on L .

We want to compare flats (q_1, L_1) and (q_2, L_2) . We set $\theta_1 = \theta(q_1, L_1)$, etc. Our main result is Corollary 6.6, proved at the end. This result will help us establish Lemma 6.3.

For each j we can rotate so that everything takes place in \mathbf{C} , and $p_j = ir_j$ and $L_j = \mathbf{R}$, and $q_j = x_j$. Here $x_j^2 + d_j^2 = r_j^2$. Suppressing the index, we have

$$D = \frac{d^2}{dx^2} E(\sqrt{d^2 + x^2}) \Big|_x = E''(r) \frac{x^2}{r^2} + \frac{E'(r)}{r} \times \frac{d^2}{r^2}. \quad (105)$$

Here E' and E'' are derivatives taken with respect to r .

Lemma 6.4 *If $\theta_2 = \theta_1$ and $r_2 \leq r_1$ and $D_1 > 0$ then $D_2 \geq D_1$.*

Proof: In our situation, there is some constant $\rho \in (0, 1]$ so that

$$\frac{r_2}{r_1} = \frac{x_2}{x_1} = \frac{d_2}{d_1} = \rho. \quad (106)$$

It follows from Equation 77 that there are constants $c \geq 1$ and $h \geq 0$ such that

$$\frac{E'(r_2)}{r_2} = c \frac{E'(r_1)}{r_1}; \quad E''(r_2) = (c + h)E''(r_1). \quad (107)$$

It now follows from Equation 105 that

$$D_2 - cD_1 = hE''(r_1) \geq 0. \quad (108)$$

Hence $D_2 \geq cD_1$ for some $c \geq 1$. The lemma follows immediately. ♠

Lemma 6.5 *If $\theta_2 \leq \theta_1$ and $r_2 = r_1$ then $D_2 \geq D_1$.*

The quantity $d(q, L)$ is monotone increasing with $\theta(q, L)$. Thus, we have $d_2 \leq d_1$. This time, we have

$$r := r_2 = r_1; \quad d_2 \leq d_1; \quad x_2 \geq x_1. \quad (109)$$

We again have Equation 105. Note that $E''(r) > 0$ and $E'(r) < 0$. When we change from the index $j = 1$ to the index $j = 2$, we do not decrease the positive coefficient of $E''(r)$ in the first term and we do not increase the positive coefficient of $E'(r)/r$ in the second term. Hence, $D_2 \geq D_1$. ♠

The previous two results combine to prove the following corollary.

Corollary 6.6 *If $\theta_2 \leq \theta_1$ and $r_2 \leq r_1$ and $D_1 \geq 0$, then $D_2 \geq D_1$.*

6.5 Proof of Lemma 6.3

We continue using the notation from above. There is a unique plane Π such that $p \cup L \subset \Pi$. We rotate the picture so that Π is the xy -plane. Let $C = S^2 \cap \Pi$. Then, as shown in Figure 6.1,

1. C is a circle whose radius is at most 1;
2. Every point of S is at least R units from p .

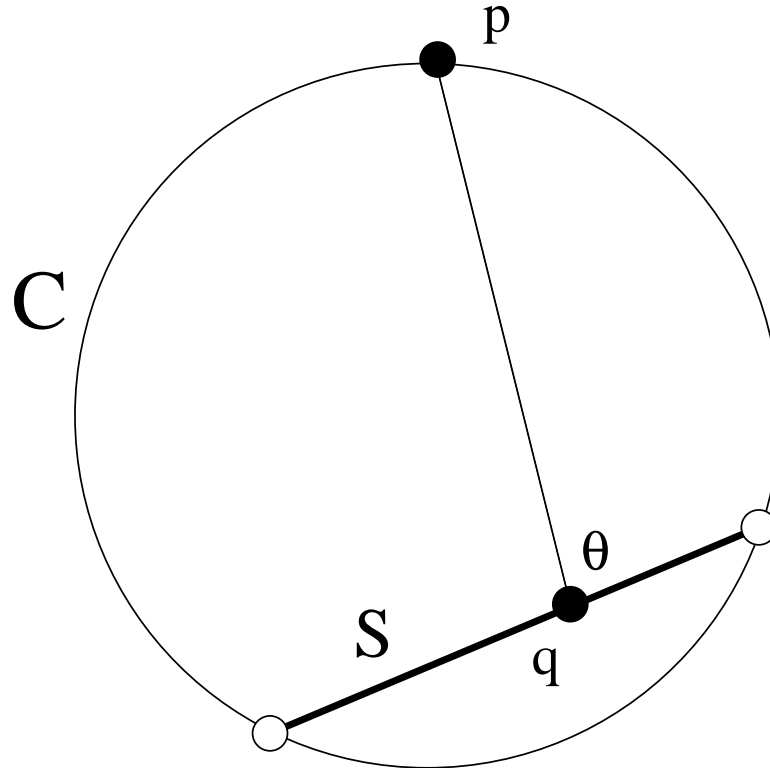


Figure 6.1: The chord and the circle

We are interested in bounding the quantity $D(q, L)$, where L is the line containing the chord S . The chord S is subject to the two constraints mentioned above. If C has radius less than 1, we replace C by a unit radius circle C' , and S by a larger segment S' such that the pair (C', S') satisfies the same constraints, and the flag (q, L') is the same as the flag (q, L) . Figure 2.2 shows the construction.

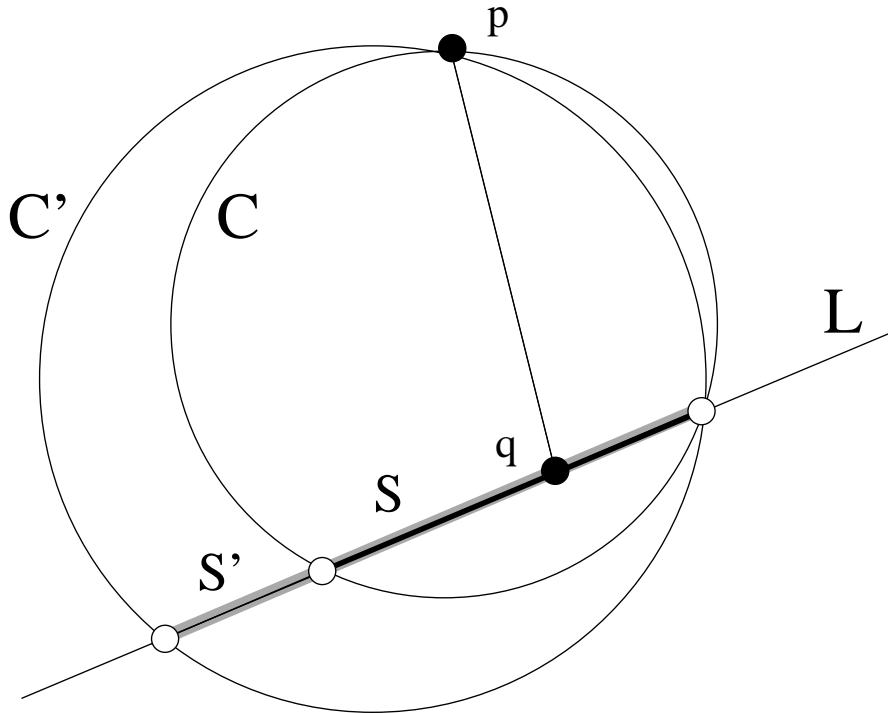


Figure 6.2: Expanding the circle

So, without loss of generality, we can assume that C is the unit circle. Also, it suffices to consider the case when $D(q, L) \geq 0$. Let $q_1 = q$. Let r_1 be the distance from p to q_1 . Note that $r_1 \geq R$. Let q_2 denote a point on C that is exactly $R = r_2$ units from p . Let L_2 be the line tangent to C at q_2 . We want to apply Corollary 6.6 to the flats (q_1, L_1) and (q_2, L_2) . We already know that $r_2 \leq r_1$.

Lemma 6.7 $\theta_2 \leq \theta_1$.

Proof: See Figure 6.3. Let q_3 be the endpoint of S such that the small angle θ_1 subtends the arc of C between p and q_3 , as shown in Figure 6.3. Let L_3 be the line tangent to C at q_3 . Let $\theta_3 = \theta(q_3, L_3)$. The angle θ_1 is half the length of the two thick arcs in Figure 6.3 whereas the angle θ_3 is half the length of the thick arc joining p to q_3 . Hence $\theta_3 \leq \theta_1$. But the angle θ_3 decreases as we move q_3 towards p along C . Therefore $\theta_2 \leq \theta_3$. Putting these two inequalities together, we find that $\theta_2 \leq \theta_1$. ♠

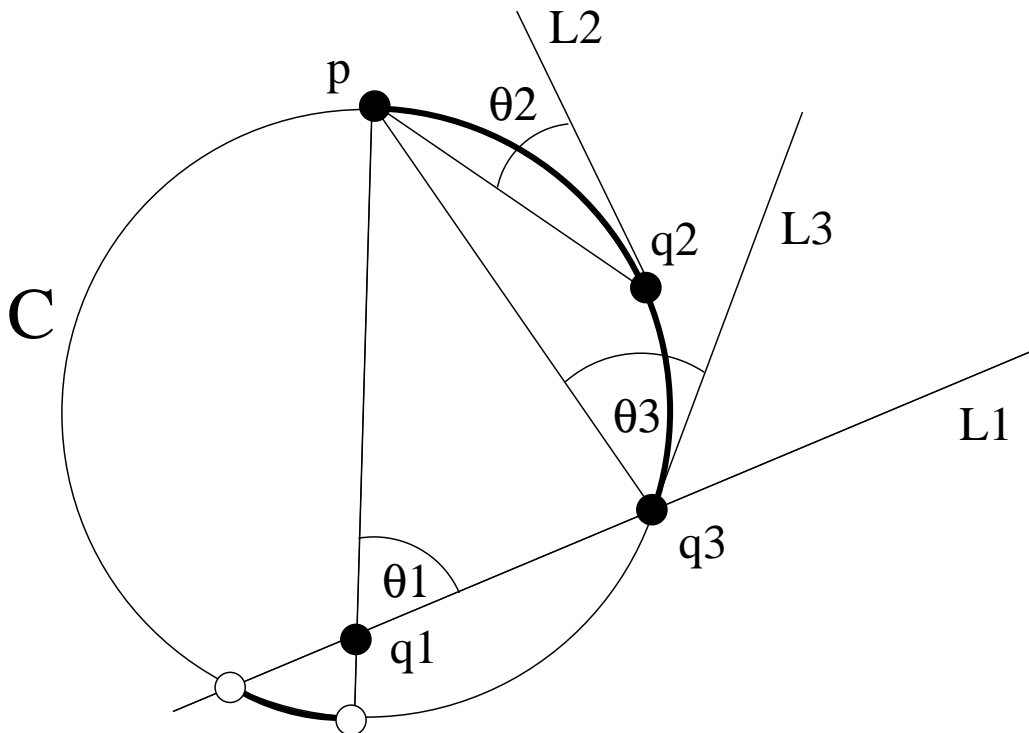


Figure 6.3: Comparing two flags.

Corollary 6.6 now says that $D(q_2, L_2) \geq D(q_1, L_1)$. To finish our proof, it remains only to compute the quantity $D(q_2, L_2)$.

We know that $r_2 = R$. Some elementary geometry shows that

$$d_2 = \frac{R^2}{2}; \quad x_2 = r^2 - d_2 \quad (110)$$

Plugging Equation 110 into Equation 105 and simplifying, we get

$$D(q_2, L_2) = \frac{R}{4}E'(R) + \left(1 - \frac{R^2}{4}\right)E''(R), \quad (111)$$

the bound from Lemma 6.3. Now we know that

$$D(q, L) \leq \frac{R}{4}E'(R) + \left(1 - \frac{R^2}{4}\right)E''(R), \quad (112)$$

for all flags (q, L) such that $\|p - q\| \geq R$. But $D(q, L)$ is just another name for the quantity $d^2\phi/ds^2$ featured in Lemma 6.3. This completes the proof of Lemma 6.3.

7 Parametrizing Arcs and Segments

7.1 Overview

Let $S \subset \mathbf{C}$ be a line segment. In this chapter we define a certain parametrization of S by a parameter $x \in [0, 1]$. Once we define our parametrization, we will state and prove several geometric results about it. As with the last chapter, the reader might want to just note the results on the first reading and then come back later for the proofs.

Let A be a circular arc on S^2 , and let A' be the chord that joins the endpoints A_0 and A_1 of A . Throughout the chapter, we assume that A is contained in a semicircle. We let $x \rightarrow A'_x$ be the affine map from $[0, 1]$ to A' . Let C be the circle containing A , and let $c \in C$ be the point which is diametrically opposed to the midpoint of A . We define A_x so that the three points c, A'_x, A_x are always collinear. Here is our first result.

Lemma 7.1 *The function $f(x) = \|A_x - A'_x\|$ attains its maximum at $x = 1/2$.*

Now we return to our main task of parametrizing a segment $S \subset \mathbf{C}$. Let $S^* = \Sigma^{-1}(S)$. The method above gives us a parametrization of S^* . Now we define

$$S_x = \Sigma(S_x^*). \quad (113)$$

As usual Σ denotes stereographic projection.

Suppose Q is a normal dyadic square. This means that Q does not cross the coordinate axes, and the side length of Q is at most 1. We consider the case when Q is contained in the positive quadrant. The other cases have symmetric treatments. Let Q_0 and Q_1 be the left and right edges of Q . For any $x \in [0, 1]$, let Q_x denote the segment connecting $(Q_0)_x$ and $(Q_1)_x$. The main result in this chapter gives estimates on the size and shape of the image of $Q_x^* = \Sigma^{-1}(Q_x)$.

Lemma 7.2 *Q_x^* has arc length at most*

$$\delta \times 1.0013.$$

and is contained in a circle of radius at least

$$\frac{1}{\sqrt{1 + \bar{y}^2}}.$$

7.2 Proof of Lemma 7.1

Our result is scale-invariant. It suffices to prove the result when A is an arc of the unit circle, as shown in Figure 7.1. The arc cy is evidently shorter than the diameter cx . On the other hand, the arc cz is evidently longer than the arc cw . Hence the arc yz is shorter than the arc wx . This is what we wanted to prove.

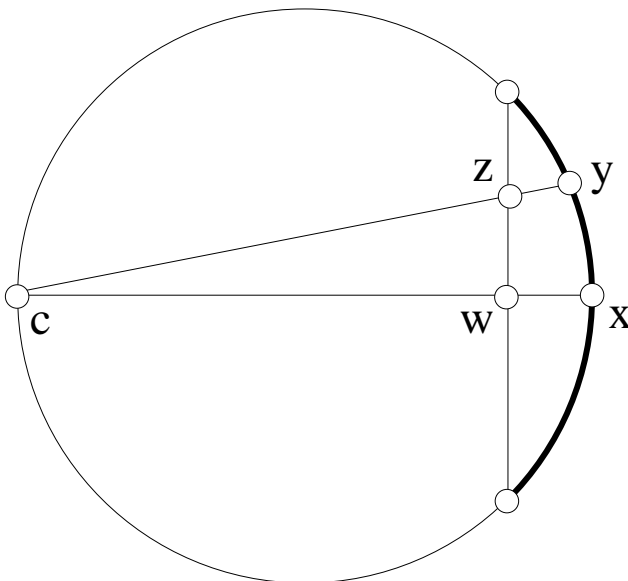


Figure 7.1: The relevant points

7.3 A Lemma about Slopes

The rest of the chapter is devoted to proving Lemma 7.2. Here we reduce Lemma 7.2 to a more geometric statement.

Lemma 7.3 Q_x has slope in $(0, 0.051)$ for all Q and $x \in (0, 1)$.

Proof of Lemma 7.2: Let $S = Q_x$. We deal first with the arc length of S^* . This is really the same argument as in Lemma 3.4. When evaluated at all points of S , the quantity in Equation 7 is at most δ/s . Since S has slope in $(0, 0.051)$ and Q has side length s , the segment S has length at most

$$s \times \sqrt{1 + (0.051)^2} < 1.0013. \quad (114)$$

The arc length estimate on S^* follows by integration.

Since the line L through S has positive slope, it intersects the imaginary axis in a point of the form iy where $y < \underline{y}$. But then, according to Equation 6, there are two points on $(L \cup \infty)^*$ which are at least

$$\frac{1}{\sqrt{1 + \bar{y}^2}}$$

apart. ♠

The rest of the chapter is devoted to proving Lemma 7.3.

7.4 Mobius Geometry

Let the vertices of Q be $Q_{00}, Q_{10}, Q_{11}, Q_{01}$, starting in the bottom left corner and going counterclockwise around. Associated to Q is an auxilliary map $\phi: [0, 1] \rightarrow [0, 1]$, defined as follows.

- The point $(1 - x)Q_{00} + xQ_{01}$ is $(Q_0)_s$ for some s .
- The point $(Q_1)_s$ is $(1 - y)Q_{10} + yQ_{11}$ for some $y = \phi(x)$.

In other words, we consider the natural map $(Q_0)_s \rightarrow (Q_1)_s$ but we precompose and postcompose with affine maps to make the domain and range equal to $[0, 1]$. Lemma 7.2 is equivalent to the statement that

$$0 < \phi(x) - x < 0.051; \quad \forall x \in (0, 1). \quad (115)$$

Given 4 distinct points $A, B, C, D \in \mathbf{R}^n$, we have the cross ratio

$$\chi(A, B, C, D) = \frac{\|A - C\| \|B - D\|}{\|A - B\| \|C - D\|}. \quad (116)$$

We say that a homeomorphism from one curve to another is *Mobius* if the map preserves cross ratios. In case the curves are line segments in the plane, a Mobius map between them is the restriction of a linear fractional transformation of $\mathbf{C} \cup \infty$.

Lemma 7.4 ϕ is *Mobius*.

Proof: Since similarities are Mobius transformations, it suffices to prove that the map $(Q_0)_s \rightarrow (Q_1)_s$ is a Mobius transformation. Stereographic projection is well known to be a Mobius map from any line segment in \mathbf{C} to the corresponding arc on S^2 . Referring to the construction in the beginning of §7.1, the map from A_x to A'_x is just the composition of affine maps with (one dimensional) stereographic projection. Hence, this map is also Mobius.

Let $A_0 = Q_0^*$ and A'_0 be the chord connecting the endpoints of A_0 . Likewise define A_1 and A'_1 . The map of interest to us is the composition

$$Q_0 \rightarrow A_0 \rightarrow A'_0 \rightarrow A'_1 \rightarrow A_1 \rightarrow Q_1. \quad (117)$$

The outer maps are Mobius, from what we have already said, and the middle map is affine. ♠

A Mobius map from $[0, 1]$ to $[0, 1]$ is completely determined by its derivative at either endpoint. Thus, we can understand ϕ by computing or estimating $\phi'(0)$. In our next result, we think of $\phi'(0)$ as a function of the choice of dyadic square Q . As in Equation 7, define

$$g(x, y) = \frac{2}{1 + x^2 + y^2}. \quad (118)$$

Define

$$G_Q = \frac{g(Q_{00})g(Q_{11})}{g(Q_{10})g(Q_{01})}. \quad (119)$$

Lemma 7.5 *Relative to Q , we have*

$$\phi'(0) = \sqrt{G_Q}.$$

In particular, ϕ is the identity iff $G_Q = 1$.

Proof: It follows from symmetry that

$$\phi'(0)\phi'(1) = 1. \quad (120)$$

Therefore

$$\phi'(0) = \sqrt{\frac{\phi'(0)}{\phi'(1)}}. \quad (121)$$

Looking at the composition in Equation 117, all the maps except the outer two have the same derivative at either endpoint. For the affine map in the middle, this is obvious: the derivative is constant. In the case of the map $A_j \rightarrow A'_j$ this follows from the fact that we are projecting from a point c_j that is symmetrically located with respect to A'_j and A_j . Call this property of the derivatives the *symmetry property*.

By Equation 7, the quantity $g(Q_{00})$ is the norm of the derivative of Σ^{-1} at Q_{00} . The other quantities $g(Q_{ij})$ have similar interpretations. It therefore follows from the symmetry property and the Chain Rule that

$$\frac{\phi'(0)}{\phi'(1)} = \frac{g(Q_{00})/g(Q_{01})}{g(Q_{10})/g(Q_{11})}. \quad (122)$$

This Lemma now follows from Equations 121 and 122. ♠

7.5 The End of the Proof

For the purposes of doing calculus, we define ϕ and G relative to any square that is contained in the positive quadrant. We remind the reader that we only consider squares that have side length at most 1.

Lemma 7.6 *It never happens that $G_Q = 1$.*

Proof: When $Q_{00} = (x, y)$ and Q has side length r , we compute

$$G_Q = \frac{(1 + r^2 + 2rx + x^2 + y^2)(1 + r^2 + 2ry + x^2 + y^2)}{(1 + x^2 + y^2)(1 + 2r^2 + x^2 + y^2 + 2rx + 2ry)} \quad (123)$$

Every factor in Equation 123 is a polynomial with only constant coefficients and at least one constant term. Hence this expression never vanishes. ♠

When $Q = [0, 1]^2$, we compute that $G_Q = 4/3$. Hence $\phi'(0) > 1$ relative to this choice of Q . It follows from continuity that $\phi'(0) > 1$ relative to any square in the positive quadrant. But this means that ϕ is increasing. (Here, of course, we are crucially using the fact that ϕ is a Mobius map from $[0, 1]$ to $[0, 1]$.) Hence $\phi(x) > x$. This proves that the slope of the segment Q_x is positive for all Q and all $x > 0$. This proves half of Lemma 7.3. Now we turn to the other half.

Lemma 7.7 *The quantity G_Q is maximized when Q has side length 1 and*

$$Q_{00} = (\xi, \xi); \quad \xi = \frac{\sqrt{3} - 1}{2}.$$

Proof: Let $\psi(x, y, r)$ be the function in Equation 123. We compute symbolically that

$$\frac{d\psi}{dr} = \frac{\Delta(x, y, r)}{(1 + x^2 + y^2)^2(1 + 2r^2 + x^2 + y^2 + 2rx + 2ry)^2}, \quad (124)$$

Where Δ is a polynomial with entirely positive terms, at least one of which involves only r . (The polynomial is rather long and unenlightening.) From this we conclude that $d\psi/dr > 0$. Hence, the maximum value of G_Q must occur when $r = 1$.

We compute that $\psi(\xi, \xi, 1) = 3/2$. So, we just have to show that the function $h(x, y) = 3/2 - \psi(x, y, 1)$ is non-negative on the positive quadrant. We compute that h is a rational function. The denominator is a polynomial with only positive terms, and the numerator N equals

$$1 - 2x + 4x^2 + 2x^3 + x^4 - 2y - 8xy + 2x^2y + 4y^2 + 2xy^2 + 2x^2y^2 + 2y^3 + y^4 \quad (125)$$

In fact, N is non-negative on the entire plane. To see this, we make the change of variables

$$x = \xi + u; \quad y = \xi + v. \quad (126)$$

With this change of variables, we find that $N - (2u - 2v)^2$ is a polynomial involving only positive terms. ♠

In light of the previous result, the quantity $\phi'(0)$ is maximized for the special square Q_0 from Lemma 7.7. Since $G = 3/2$ in this case, we have

$$\phi'(0) = \sqrt{3/2}. \quad (127)$$

But this equation pins down ϕ uniquely, and we observe that the map

$$\phi(x) = \frac{3\sqrt{2}x}{2\sqrt{3} + 3\sqrt{x} - 2\sqrt{3}x}. \quad (128)$$

has the same derivative. Hence, this is the correct formula for ϕ . A bit of calculus now shows that

$$\phi(x) - x < 0.051; \quad \forall x \in [0, 1]. \quad (129)$$

This completes the proof.

8 Proof of Lemma 5.2

8.1 The Geometry of Circles

We need one more result about circles.

Lemma 8.1 *Suppose that A is an arc of a circle C . Let d be the arc-length of A . Let A' be the segment connecting the endpoints of A . Let r be the radius of C . Let μ be the smallest constant such that every point of A is within μ of some point of A' . Then*

$$\mu < \frac{d^2}{8r}.$$

Proof: Let's first consider the case $r = 1$. We rotate so that C is the unit circle, and A is the arc bounded by the points $\exp(-i\theta)$ and $\exp(i\theta)$. Here $\theta \in (0, \pi)$. Then

$$d = 2\theta; \quad \mu = 1 - \cos(\theta). \quad (130)$$

The claim of this lemma boils down to the statement that

$$\frac{\theta^2}{1 - \cos(\theta)} > 2, \quad (131)$$

This is equivalent to the statement that

$$\phi(\theta) = \theta^2 + 2 \cos(\theta) - 2 > 0. \quad (132)$$

We have $\phi(0) = 0$ and

$$\phi'(\theta) = 2(\theta - \sin(\theta)) > 0. \quad (133)$$

This proves what we need.

If $r \neq 1$, we let T be a dilation that scales distances by a factor of $1/r$. The arc $T(A)$ has length d/r and $T(C)$ has radius 1. We apply our result to the pair $(T(A), T(C))$ and find that every point of $T(A)$ is within

$$\frac{(d/r)^2}{8}$$

of $T(C)$. Applying T^{-1} , we get the desired result for the pair (A, C) . ♠

8.2 Lemma 5.2 for dyadic segments

8.2.1 Defining the Weighting

Suppose that (Q, \widehat{Q}) is a reasonable pair, and Q is a dyadic line segment. The construction in the previous chapter gives us a parametrization $x \rightarrow Q_x$. We take Q_0 to be the left endpoint and Q_1 to be the right endpoint. The corresponding endpoints of Q^* are Q_0^* and Q_1^* . We define our weighting as follows. Letting $z = Q_x$, we define

$$\lambda_0(z) = 1 - x; \quad \lambda_1(z) = x; \quad (134)$$

8.2.2 Setting up the Calculation

To bring our notation in line with Lemma 6.1, we define

$$A = A(Q_0^*, Q_1^*) = Q^*; \quad A' = A'(Q_0^*, Q_1^*). \quad (135)$$

Let $(z, w) \in Q \times \widehat{Q}$. Define

$$p = \Sigma^{-1}(w); \quad q = \Sigma^{-1}(z). \quad (136)$$

Setting $x = \lambda_1(z)$, we have

$$q = A_x. \quad (137)$$

We also define

$$q' = A'_x \quad (138)$$

The idea of our proof is to estimate things with q' in place of q , and then to estimate the error we get when replacing q' by q .

8.2.3 Using Lemma 6.1

Let F be as in Equation 98. We have

$$\begin{aligned} \sum_u \lambda_u(z) f(Q_u, w) &= (1 - x)F(A'_0) + xF(A'_1); \\ F(A'_x) &= E(\|q' - p\|). \end{aligned} \quad (139)$$

Lemma 6.1 now tells us that

$$\sum_u \lambda_u(z) f(Q_u, w) - E(\|p - q'\|) \leq \max(0, \Lambda_1) \delta^2 \quad (140)$$

8.2.4 The Easy Case

Now we need to see what happens when we replace q' by q . Define

$$r = \|p - q\| \quad r' = \|p - q'\|. \quad (141)$$

If $r' \geq r$ then (since E is decreasing)

$$E(\|p - q\|) \geq E(\|p - q'\|). \quad (142)$$

In this case, our proof is done: Equations 142 and 140 combine to give a tighter bound than what Lemma 5.2 gives.

8.2.5 The Hard Case

Now suppose $r' < r$. Since E is convex, E' is monotone decreasing. Therefore

$$E(r') - E(r) \leq E'(r')\|q - q'\| \leq E'(R)\|q - q'\|. \quad (143)$$

Here $R \geq r'$ is as in Lemma 5.2.

The same proof as in Lemma 7.2 shows that A has arc length at most δ . Also A is contained in a great circle – i.e. a circle of radius 1. Lemma 8.1 now says that every point of A is within $\delta^2/8$ of A' . But the point of A' closest to $A_{1/2}$ is $A'_{1/2}$. Therefore

$$\|q - q'\| = \|A_x - A'_x\| \leq^* \|A_{1/2} - A'_{1/2}\| \leq \frac{\delta^2}{8}. \quad (144)$$

The starred inequality is Lemma 7.1. Combining Equations 143 and 144, we find that

$$E(r') - E(r) \leq E'(R)\frac{\delta^2}{8} = \Lambda_2 \delta^2. \quad (145)$$

Note that

$$f(z, w) = E(\|p - q\|). \quad (146)$$

Hence, by Equation 146,

$$E(\|p - q'\|) - f(z, w) = E(r') - E(r) \leq \Lambda_2 \delta^2. \quad (147)$$

Adding Equations 140 and 147, we get the bound in Lemma 5.2. This completes the proof in case Q is a dyadic segment.

8.3 The Weighting for Dyadic Squares

Let Q be a dyadic square and let $Q^* = \Sigma^{-1}(Q)$. Let Q_{ab} be the vertices of Q , as in §7.4. Let Q_{ab}^* be the corresponding vertex of Q^* . As we make our construction, the reader should picture the letter ‘H’, with the horizontal bar very slightly slanted. We will use coordinates $(h, v) \in [0, 1]^2$. The v variable moves along vertical segments and the h variable moves along (roughly) horizontal segments.

Let Q_0 be the left edge of Q . The two endpoints of Q_0 are Q_{00} and Q_{01} . Likewise, let Q_1 be the right edge of Q . The two endpoints of Q_1 are Q_{10} and Q_{11} . Using the parametrization from the previous chapter, we define

$$Q_{0v} = (Q_0)_v \in Q_0; \quad Q_{1v} = (Q_1)_v \in Q_1. \quad (148)$$

Next, we define Q_v to be the segment joining Q_{0v} to Q_{1v} . Note that Q_v is nearly horizontal but not exactly horizontal. See Lemma 7.3. Finally, we define

$$Q_{hv} = (Q_v)_h, \quad (149)$$

again using the parametrization discussed in the previous sections. We define our weighting as follows. Assuming that $z = Q_{vh}$,

$$\begin{aligned} \lambda_{00}(z) &= (1-h)(1-v); & \lambda_{10}(z) &= (h)(1-v); \\ \lambda_{01}(z) &= (1-h)(v); & \lambda_{11}(z) &= (h)(v). \end{aligned} \quad (150)$$

In the previous section, we defined a weighting for dyadic segments. We could equally well define this weighting for any segment, since we have already explained how to parametrize any such segment. There are three ways in which our weighting here is compatible with the weighting for segments.

- With respect to the segment Q_0 , the weighting for the point S_{0v} is $\lambda_0 = 1 - v$ and $\lambda_1 = v$.
- With respect to the segment Q_1 , the weighting for the point S_{1v} is $\lambda_0 = 1 - v$ and $\lambda_1 = v$.
- With respect to the segment Q_v , the weighting for the point Q_{hv} is $\lambda_0 = 1 - h$ and $\lambda_1 = h$.

8.4 The End of The Proof

For ease of notation, we will assume that our dyadic square lies in the positive quadrant. The other cases are similar, and indeed follow from symmetry. We gather 4 pieces of information.

1. The circles containing the arcs Q_0^* and Q_1^* have radius at least

$$\frac{1}{\sqrt{1+\bar{x}}}.$$

This follows from Equation 6 and from the fact that the line extending a vertical edge of Q comes within \bar{x} of the origin.

2. The arcs Q_0^* and Q_1^* have length at most δ . This follows from the same argument as in Lemma 7.2.
3. For any $v \in [0, 1]$, the line extending the segment Q_v comes within \bar{y} of the origin. Hence, the circle containing Q_v^* has radius at least

$$\frac{1}{\sqrt{1+\bar{y}}}.$$

See Lemma 7.2.

4. For any $v \in [0, 1]$, the arc Q_v^* has length at most $(1.0013) \times \delta$. See Lemma 7.2.

Now we are ready for the main argument. The basic idea is to make repeated appeals to the segment case of Lemma 5.2 and then to suitably average the result.

We define

$$\begin{aligned} \Lambda_{1x} &= \Lambda_{1y} = \Lambda_1/2; \\ \Lambda_{2x} &= -\frac{E'(R)}{8}\sqrt{1+\bar{x}^2}; & \Lambda_{2y} &= -\frac{E'(R)}{7.98}\sqrt{1+\bar{y}^2}. \end{aligned} \quad (151)$$

We have

$$\Lambda_1 = \Lambda_{1x} + \Lambda_{1y}; \quad \Lambda_2 = \Lambda_{2x} + \Lambda_{2y}. \quad (152)$$

Let $p \in (\widehat{Q})^*$ be some point. Let $w = \Sigma(p)$. Let f be as in Lemma 5.2. That is

$$f(z, w) = E(\|\Sigma^{-1}(z) - \Sigma^{-1}(w)\|). \quad (153)$$

Applying the segment case of Lemma 5.2 to the arc Q_0 , we find that

$$Z_1 := (1-v)f(Q_{00}, w) + vf(Q_{01}, w) - f(Q_{0v}, w) \leq \left(\max \Lambda_{1x} + \Lambda_{2x} \right) \delta^2 \quad (154)$$

The proof is exactly the same as in the previous section, except for the one point that the circular arc Q_0^* lies not necessarily in a great circle but rather a circle whose radius is bounded by Item 1 above. The designation Z_1 is for algebraic purposes which will become clear momentarily. Similarly

$$Z_2 := (1-v)f(Q_{10}, w) + vf(Q_{11}, w) - f(Q_{1v}, w) \leq \left(\max \Lambda_{1x} + \Lambda_{2x} \right) \delta^2 \quad (155)$$

Finally, an argument just like the one given for *dyadic* segments also works for the segment Q_s . The only property we used about dyadic segments is that they don't cross the coordinate axes, and Q_s has this property. Using Items 3 and 4 above in place of Items 1 and 2, the same argument gives

$$Z_3 := (1-h)f(Q_{0v}, w) + hf(Q_{1v}, w) - f(Q_{hv}, w) \leq \left(\max \Lambda_{1y} + \Lambda_{2y} \right) \delta^2 \quad (156)$$

The key point here is that

$$7.98 < 8/1.0013.$$

The number 1.0013 comes up in Item 4 above.

Concentrating on the left hand sides of Equations 154, 155, and 156, we have

$$\begin{aligned} (1-h)Z_1 + hZ_2 + Z_3 = & \\ (1-h)(1-v)f(Q_{00}, w) + (1-h)(v)f(Q_{01}, w) + & \\ (h)(1-v)f(Q_{10}, w) + (h)(v)f(Q_{11}, w) - f(Q_{hv}, w) = & \\ \left(\sum_{ab} \lambda_{ab}(z) f(Q_{ab}, w) \right) - f(z, w); \quad z = Q_{hv}. & \quad (157) \end{aligned}$$

Concentrating on the right hand sides, we see that the quantity in Equation 157 is at most

$$\begin{aligned} (1-h) \left(\max \Lambda_{1x} + \Lambda_{2x} \right) \delta^2 + (h) \left(\max \Lambda_{1x} + \Lambda_{2x} \right) \delta^2 + \left(\max \Lambda_{1y} + \Lambda_{2y} \right) \delta^2 = & \\ \left(\max(\Lambda_1, 0) + \Lambda_2 \right) \delta^2. & \quad (158) \end{aligned}$$

This proves Lemma 5.2.

9 The Hessian and its Variation

9.1 Main Part of the Proof

In this chapter we prove Lemma 2.4. Let H_e denote the Hessian of \mathcal{E} , the energy function, relative to the function $E(r) = r^{-e}$. Let Z be the configuration corresponding to the TBP, normalized as in Equation 30.

Lemma 9.1 *The lowest eigenvalue of H_e exceeds $1/10$ for $e = 1, 2$.*

Proof: Let M be either of the two matrices. Let I_7 be the 7×7 identity matrix. Using a modified version of the Cholesky Decomposition, as discussed in [Wa, p 84], we write

$$\left(M - \frac{1}{10}I_7\right) = LDL^t. \quad (159)$$

where L is lower triangular, D is diagonal matrix with all diagonal entries positive, and L^t is the transpose of L . This suffices to show that $M - \frac{1}{10}I_7$ is positive definite. Hence, the lowest eigenvalue of M is at least $1/10$. ♠

Given a square matrix M , we define

$$\|M\|_2 = \left(\sum_{i,j} M_{ij}^2\right)^{1/2}. \quad (160)$$

We mention a familiar and useful property of this norm.

Lemma 9.2 *For any unit vector $v \in \mathbf{R}^7$ we have $\|M(v) \cdot v\| \leq \|M\|_2$.*

Proof: We have

$$\begin{aligned} \|M(v) \cdot v\|_2 &= \left\| \sum M_{ij} v_i v_j \right\|_2 \leq^* \|M\|_2 \left\| \sum (v_i v_j)^2 \right\|^{1/2} = \\ & \|M\|_2 \sqrt{\left(\sum v_i^2\right)\left(\sum v_j^2\right)} = \|M\|_2 \|v\|^2 = \|M\|_2. \end{aligned} \quad (161)$$

The starred inequality is the Cauchy-Schwarz inequality. ♠

We write $M' \prec M$ if $|M'_{ij}| \leq M_{ij}$ for all indices. Recall that $s = 2^{-11}$, as in Lemmas 2.3 and 2.4. Let D_k denote the partial derivative with respect to the k th direction in \mathbf{R}^7 .

Lemma 9.3 (Variation Bound) Let $\Psi_{1,e}, \dots, \Psi_{7,e}$ be the smallest non-negative matrices such that $D_k H_e(Z) \prec \Psi_{k,e}$ for all k and all $Z \in \Omega_s$. Let

$$\Psi(e) = \left\| \sum_{k=1}^7 \Psi_{k,e} \right\|_2.$$

Then $\Psi(1) < 345$ and $\Psi(2) < 140$ and, $\sup_e \Psi(e) < 463$.

Corollary 9.4 Let Z be the center of Ω_s (i.e., the TBP) and let $W \in \Omega_s$ be any other point. Then

$$\|H_e(Z) - H_e(W)\|_2 < \frac{1}{10}; \quad \forall e \in (0, \infty).$$

Proof: Let $H = H_e$. Say that a *special path* in Ω is a 7-segment polygonal path γ such that the i th segment is parallel to the i th coordinate direction. We can connect $Z = Z_0$ to $W = Z_7$ by a special path γ , all of whose segments have length at most 2^{-12} . Let Z_0, \dots, Z_7 be the vertices of γ . Let $\Delta_{ij} = H(Z_i) - H(Z_j)$. Integrating along the k th segment, we get the bound $\Delta_{k,k-1} \prec 2^{-12} \Psi_k$. Hence

$$\|H(Z) - H(W)\|_2 = \|\Delta_{70}\|_2 = \left\| \sum_{k=1}^7 \Delta_{k,k-1} \right\|_2 \leq \frac{\left\| \sum_{k=1}^7 \Psi_k \right\|_2}{2^{12}} < \frac{345}{4096}. \quad (162)$$

This last quantity is less than $1/10$. ♠

Proof of Lemma 2.4: Let $e = 1$ or $e = 2$. Let $H = H_e$. Let $W \in \Omega_s$ be some point. We want to show that $H(W)$ is positive definite. Let $A = H(Z)$ and $B = H(W)$. By the preceding Corollary, we have $B = A + \Delta$ with $\|\Delta\|_2 < 1/10$.

Now let $v \in \mathbf{R}^7$ be any unit vector. We have

$$Bv \cdot v = Av \cdot v + \Delta v \cdot v \geq Av \cdot v - |\Delta v \cdot v| > \frac{1}{10} - \|\Delta\|_2 > 0. \quad (163)$$

Hence B is positive definite. The fact that $Av \cdot v > 1/10$ comes from the fact that the lowest eigenvalue of the symmetric matrix A is greater than $1/10$. ♠

9.2 A Stronger Bound

Consider the function

$$\phi(x) = x^{e/2} \tag{164}$$

and the interval

$$I = \left[\frac{1}{4} + \frac{1}{2} + 2^{-9} \right]. \tag{165}$$

Define

$$c_k(e) = \sup_{x \in I} \frac{d^k \phi}{dx^k}(x) \tag{166}$$

Setting $c_k = c_k(e)$, we define

$$\Upsilon(e) = \sqrt{19336c_1^2 + 19036c_1c_2 + 4922c_2^2 + 1474c_1c_3 + 772c_2c_3 + 31c_3^2}. \tag{167}$$

Our next result uses the notation from the Variation Bound.

Lemma 9.5 (Variation Bound II) $\Psi(e) < \Upsilon(e)$ for all $e \in (0, \infty)$.

We find easily that

$$(c_1(1), c_2(1), c_3(1)) = (1, 2, 12). \tag{168}$$

Plugging this into Equation 167, we get $\Psi(1) < 345$. Similarly, we have

$$(c_1(2), c_2(2), c_3(2)) = (1, 0, 0). \tag{169}$$

This yields $\Psi(2) < 140$.

Some elementary calculus shows that

$$\sup_{e \in (0, \infty)} c_1(e) < 1.1; \quad \sup_e c_2(e) < 3.2; \quad \sup_{e \in (0, \infty)} c_3(e) < 16. \tag{170}$$

We omit the details, because we don't use the general bounds anywhere in our main proof. When we plug in these bounds we find that $\Psi(e) < 463$ for all e . Hence, the Variation Bound II implies the Variation Bound.

Remark: The Variation Bound II is generally much better than the Variation Bound. For instance, $\Upsilon(e) \rightarrow 0$ as $e \rightarrow 0$ or as $e \rightarrow \infty$.

9.3 Proof of the Variation Lemma II

Our proof usually suppresses the dependence on the exponent e .

A point $(z_0, z_1, z_2, z_3) \in \Omega_s$ is such that each z_m lies within a square Δ_{m+1} of side length 2^{-11} about one of the points of the TBP configuration, normalized as in Equation 30. Let R_1 be the union of these 4 squares, $\Delta_1, \dots, \Delta_4$. Let $R_2 \subset \mathbf{C}^2$ denote the set of points z_1, z_2 which arise as a disjoint pair of finite points of a configuration of Ω_s . Here R_2 consists of 12 components, all of the form $\Delta_i \times \Delta_j$. The components $\Delta_i \times \Delta_j$ and $\Delta_j \times \Delta_i$ are *partners*. We let $\Delta_5, \dots, \Delta_{10}$ be 6 components, no two of which are partners.

Recall that Σ^{-1} is inverse stereographic projection. See Equation 5. Setting $z = x + iy$, define

$$F(z) = \frac{1}{\|\Sigma^{-1}(z) - \Sigma^{-1}(\infty)\|^2} = \frac{1 + x^2 + y^2}{4}. \quad (171)$$

$$G(z_1, z_2) = \frac{1}{\|\Sigma^{-1}(z_1) - \Sigma^{-1}(z_2)\|^2} = \frac{(1 + x_1^2 + y_1^2)(1 + x_2^2 + y_2^2)}{4(x_1 - x_2)^2 + (y_1 - y_2)^2}. \quad (172)$$

Let ϕ be as in Equation 164. According as $m \leq 4$ or $m \geq 5$, define

$$\widehat{U}_m = \phi \circ U_m; \quad U_m = F \text{ or } G \quad (173)$$

Define

$$\Phi(i, j, k, m) = \sup_{\Delta_m} |D_i D_j D_k U_m|; \quad \widehat{\Phi}(i, j, k, m) = \sup_{\Delta_m} |D_i D_j D_k \widehat{U}_m|. \quad (174)$$

Here $i, j, k \in \{1, \dots, 7\}$ and $m \in \{1, \dots, 10\}$ and D_k is the k th partial derivative.

We have

$$\mathcal{E}(z_0, z_1, z_2, z_3) = \sum_{m=1}^{10} \widehat{U}_m, \quad (175)$$

where the arguments of the functions on the right hand side are suitably chosen sub-lists of (z_0, z_1, z_2, z_3) . Therefore

$$|D_k D_i D_j(\mathcal{E})| \leq \Psi_k(i, j) := \sum_{m=1}^{10} \widehat{\Phi}(i, j, k, m). \quad (176)$$

With this definition of Ψ_k , we have $D_k H \prec \Psi_k$. Summing over k , we have

$$\left\| \sum_{k=1}^7 \Psi_k \right\|_2 \leq \left\| \sum_{k,m} \widehat{\Phi}(i, j, k, m) \right\|_2. \quad (177)$$

Say that $i \in \{1, \dots, 7\}$ is *related* to an index $m \in \{1, \dots, 10\}$ if a change in the coordinate x_i moves one of the points in the argument of \widehat{U}_m . For instance $i = 2$ is related to $m = 5$ because changing x_2 changes the location of the point $z_1 = x_1 + ix_2$, and the argument of U_5 is the point $(z_0, z_1) \in \Delta_5$. Clearly $\widehat{\Phi}(i, j, k, m) = 0$ unless i, j, k are all related to m .

When all indices are related to m , we use the chain rule

$$\begin{aligned} D_i D_j D_k \widehat{U}_m &= \phi' \times D_i D_j D_k U_m + \phi''' \times D_i U_m \times D_j U_m \times D_k U_m + \\ &\phi'' \times D_i D_j U_m \times D_k U_m + \phi'' \times D_j D_k U_m \times D_i U_m + \phi'' \times D_k D_i U_m \times D_j U_m. \end{aligned} \quad (178)$$

Given the definitions of the regions R_1 and R_2 we have $U_m(\Delta_m) \subset I$, where I is the interval from Equation 165. Combining this fact with Equation 166 and Equation 178, we have

$$\begin{aligned} \widehat{\Phi}(i, j, k, m) &\leq c_1 \Phi(i, j, k, m) + c_3 \Phi(i, m) \Phi(j, m) \Phi(k, m) + \\ &c_2 \Phi(i, j, m) \Phi(k, m) + c_2 \Phi(j, k, m) \Phi(i, m) + c_2 \Phi(k, i, m) \Phi(j, m). \end{aligned} \quad (179)$$

Let δ_m be the center of Δ_m . Define

$$a(i, j, k, m) = |D_i D_j D_k U_m(\delta_m)|. \quad (180)$$

We define $a(i, j; m)$ and $a(i; m)$ similarly. Define

$$v = ((v(i), v(i, j), v(i, j, k))) = \left(\frac{1}{1000}, 0, 0 \right) \quad \text{or} \quad \left(\frac{1}{200}, \frac{1}{50}, \frac{1}{10} \right), \quad (181)$$

according as $m \leq 4$ or $m \geq 5$. Let $b(i; m) = a(i; m) + v(i)$, etc.

Lemma 9.6 *for all (i, j, k, m) we have*

$$\Phi(i, m) \leq b(i, m); \quad \Phi(i, j, m) \leq b(i, j, m); \quad \Phi(i, j, k, m) \leq b(i, j, k, m).$$

Combining Equation 177, Equation 179, and Lemma 9.6, we have

$$\sum_k \Psi_k \prec \sum_{k,m} \delta(i, j, k, m) \begin{pmatrix} c_1 b(i, j, k, m) + \\ c_2(b(i, j, m)b(k, m) + \\ c_2(b(j, k, m)b(i, m) + \\ c_2(b(k, i, m)b(j, m) + \\ c_3 b(i, m)b(j, m)b(k, m) \end{pmatrix} \quad (182)$$

Here $\delta(i, j, k, m) = 1$ if i, j, k are all related to m , and otherwise 0. When we compute the norm of the right hand side in Mathematica, we get the square root of a polynomial in c_1, c_2, c_3 . Rounding the coefficients of this polynomial up to integers, we get Υ . This completes the proof of the Variation Bound II, modulo the proof of Lemma 9.6.

9.4 Proof of Lemma 9.6

When $m \leq 4$, we are dealing with the function F from Equation 171. We have $D_i F = x_i/2$ and all higher derivatives are constant. Lemma 9.6 in this trivial case now follows from the fact that $\text{radius}(\Delta_m) < 1/500$.

For the nontrivial cases, we fix some value of $m \in \{5, \dots, 10\}$ and consider the cube $\Delta = \Delta_m \subset \mathbf{C}^2$. This cube has side-length 2^{-11} . The center point is $\delta = \delta_m$. Define

$$a_k = |\mathbf{D}_k G(\delta)|; \quad \Phi_k = \max_{(z_1, z_2) \in \Delta} |\mathbf{D}_k G(z_1, z_2)|. \quad (183)$$

The maxima here are taken over all k th partial derivatives \mathbf{D}_k . An exact, finite calculation, done for each of the 6 choices of m , yields

$$a_1 \leq 1; \quad a_2 \leq 4; \quad a_3 \leq 18; \quad a_4 \leq 96; \quad a_5 \leq 600. \quad (184)$$

Now we give an estimate on Φ_6 . Given a polynomial $P \in \mathbf{R}[x_1, y_1, x_2, y_2]$, let $|P|$ denote the sum of the absolute values of the coefficients of P . We have the easy upper bound

$$|P(z_1, z_2)| \leq |P| \max(|z_1|, |z_2|)^d; \quad d = \text{degree}(P). \quad (185)$$

Here we have set $z_j = x_j + iy_j$. Calculating symbolically we find that each 6th partial derivative D_6 has the following structure. There is a polynomial P , depending on the choice of derivative, such that

$$D_6 G = \frac{P}{\|z_1 - z_2\|^7}; \quad |P| \leq 4519440; \quad \deg(P) \leq 10. \quad (186)$$

We (easily) have

$$\max(\|z_1\|, \|z_2\|, \|z_1 - z_2\|^{-1}) < 1 + 2^{-8}; \quad \forall (z_1, z_2) \in \Delta. \quad (187)$$

Hence

$$\Phi_6 \leq 4519440 \times (1 + 2^{-8})^{17} < 5000000. \quad (188)$$

Lemma 9.7 $\Phi_k < a_k + 2^{-10} \times \Phi_{k+1}$.

Proof: Let (w_1, w_2) be a point of Δ . We can connect (w_1, w_2) to a point $(z_1, z_2) \in \delta_2$ by a 4-segment polygonal path γ such that the i th segment has length at most 2^{-12} and moves in the i th coordinate direction. This lemma now follows from integration. ♠

Now we apply Lemma 9.7 in an iterative way.

$$\Phi_5 \leq 600 + 5000000 \times 2^{-10} < 5483 \quad (189)$$

$$\Phi_4 \leq 96 + 5483 \times 2^{-10} < 102. \quad (190)$$

$$|\Phi_3 - a_3| < 102 \times 2^{-10} < \frac{1}{10}; \quad \Phi_3 < 18.1 \quad (191)$$

$$|\Phi_2 - a_2| < 18.1 \times 2^{-10} < \frac{1}{50}; \quad \Phi_2 < 4.02. \quad (192)$$

$$|\Phi_1 - a_1| \leq 4.02 \times 2^{-10} < \frac{1}{200}. \quad (193)$$

The R.H.S. of Equation 191 comes from the L.H.S. and Equation 184. Likewise, the R.H.S. of Equation 192 comes from the L.H.S. and Equation 184. This completes the proof of Lemma 9.6.

10 Computational Issues

10.1 General Remarks

Our calculations in this paper are of two kinds. The material in §9 makes some exact calculations in Mathematica [W] and the rest of the paper makes calculations in Java. For the Mathematica calculations, we need to take derivatives of rational functions or their square roots, and evaluate them at elements of $\mathbf{Q}[\sqrt{3}]$. We also need to simplify and group terms of some polynomials. Everything is manipulated exactly. The user who downloads our Java program will also find our Mathematica files in the same directory.

The bulk of the calculations are done in Java, and these are what we discuss below. We take the IEEE-754 standards for binary floating point arithmetic [I] as our reference for the Java calculations. This 1985 document has recently been superseded by a 2008 publication [I2]. We will stick to the 1985 publication for three reasons. First, the 1985 version is shorter and simpler. Second, the portion relevant to our computation has not changed in any significant way. Third, we think that some of the computers running our code will have been manufactured between 1985 and 2008, thus conforming to the older standard.

10.2 Doubles

With a view towards explaining interval arithmetic, we first describe the way that Java represents real numbers. Our Java code represents real numbers by *doubles*, in a way that is an insignificant modification of the scheme discussed in [I, §3.2.2]. To see what our program does, read the documentation for the `longBitsToDouble` method in the `Double` class, on the website <http://java.sun.j2se/1.4.2.docs/api>. According to this documentation – and experiments verify that it works this way on our computer – our program represents a double by a 64 bit binary string, where

- The first bit is called s .
- The next 11 bits are a binary expansion of an integer e .
- If $e = 0$, the last 52 bits are the binary expansion of an integer m .
- If $e \neq 0$, the last 52 bits are binary expansion of the number $m - 2^{52}$.

The real number represented by the double is

$$(-1)^s \times 2^{e-1075} \times m. \tag{194}$$

Example: The double representing -317 is stored as the 64 bit string

$$1/10000000111/001111010\dots 0.$$

The slashes are put in to emphasize the breaks. Here $s = 1$ and (since $e \neq 0$)

$$e = 2^{10} + 8 + 4 + 1 = 1031.$$

There are 44 zeros at the end of the word, and

$$m = 2^{44}(0 + 0 + 32 + 16 + 8 + 4 + 0 + 1) + 2^{52} = 2^{44}(317).$$

Hence

$$(-1)^s \times 2^{e-1075} \times m = -317.$$

Now we come to the main point of our discussion above. The non-negative doubles have a lexicographic ordering, and this ordering coincides with the usual ordering of the real numbers they represent. The lexicographic ordering for the non-positive doubles is the reverse of the usual ordering of the real numbers they represent. To *increment* x_+ of a positive double x is the very next double in the ordering. This amounts to treating the last 63 bits of the string as an integer (written in binary) and adding 1 to it. With this interpretation, we have $x_+ = x + 1$. We also have the decrement $x_- = x - 1$. Similar operations are defined on the non-positive doubles. These operations are not defined on the largest and smallest doubles, but our program never encounters (or comes anywhere near) these.

10.3 The Basic Operations

Let \mathbf{D} be the set of all doubles. Let

$$\mathbf{R}_0 = \{x \in \mathbf{R} \mid |x| \leq 2^{30}\} \tag{195}$$

Our choice of 2^{30} is an arbitrary but convenient cutoff. Let \mathbf{D}_0 denote the set of doubles representing reals in \mathbf{R}_0 .

According to the discussion in [I, 3.2.2, 4.1, 5.6], there is a map $\mathbf{R}_0 \rightarrow \mathbf{D}_0$ which maps each $x \in \mathbf{R}_0$ to some $[x] \in \mathbf{D}_0$ which is closest to x . In case

there are several equally close choices, the computer chooses one according to the method in [I, §4.1]. This “nearest point projection” exists on a subset of \mathbf{R} that is much larger than \mathbf{R}_0 , but we only need to consider \mathbf{R}_0 . We also have the inclusion $r : \mathbf{D}_0 \rightarrow \mathbf{R}_0$, which maps a double to the real that it represents.

Our calculations use the 5 functions

$$+; \quad -; \quad \times; \quad \div; \quad \sqrt{}. \quad (196)$$

These operations act on \mathbf{R}_0 in the usual way. Operations with the same name act on \mathbf{D}_0 . Regarding the first 5 basic operations, [I, §5] states that *each of the operations shall be performed as if it first produced an intermediate result correct to infinite precision and with unbounded range, and then coerced this intermediate result to fit into the destination’s format*. Thus, for doubles x and y .

$$\sqrt{x} = \left[\sqrt{r(|x|)} \right]; \quad x * y = [r(x) * r(y)]; \quad * \in \{+, -, \times, \div\}. \quad (197)$$

The operations on the left hand side represent operations on doubles and the operations on the right hand side represent operations on reals.

Remark: Exceptions to Equation 197 can arise if we divide by 0 or a number too close to zero. This will produce an *overflow error* – too large a number to be accurately represented by a double. To see that this never happens, we check that we never divide by a number smaller than 2^{-11} . Moreover, as we discuss at the end of this chapter, we never take the square root of a number less than 2^{-5} .

10.4 Interval Arithmetic

An *interval* is a pair $I = (x, y)$ of doubles with $x \leq y$. Say that I *bounds* $z \in \mathbf{R}_0$ if $x \leq [z] \leq y$. This is true if and only if $x \leq z \leq y$. Define

$$[x, y]_o = [x_-, y_+]. \quad (198)$$

This operation is well defined for doubles in \mathbf{D}_0 . We are essentially *rounding out* the endpoints of the interval. Let I_0 and I_1 denote the left and right endpoints of I . Letting I and J be intervals, we define

$$I * J = \left(\min_{ij} I_i * J_j, \max_{ij} I_i * J_j \right)_o; \quad \sqrt{I} = (\sqrt{I_0}, \sqrt{I_1})_o \quad (199)$$

That is, we perform the operations on all the endpoints, order the results, and then round outward. Given Equation 197, we have the following facts.

1. If I bounds x and J bounds y then $I * J$ bounds $x * y$.
2. If $I > 0$ bounds $x > 0$ then \sqrt{I} bounds \sqrt{x} .

After we have defined intervals and their basic operations, we define other Java objects based on intervals. Namely, interval versions of complex numbers, vectors in \mathbf{R}^3 , dyadic segments and squares, and dyadic boxes. For instance, the interval version of a complex number is an object of the form $X + iY$, where X and Y are intervals. The algebra of these interval objects – e.g. complex addition or the dot product – is formally the same as the corresponding algebra on the usual objects. At every step of the calculation, the real version of the object is bounded, component by component, by the interval version. If some particular interval object passes our test, it means that all the real objects bounded by it also pass.

10.5 Implementation Details

We implement the interval arithmetic in a way that tries to minimize the time we spend using it. We run the floating point algorithm until we notice that a box has passed one of the floating point tests. Then, we re-perform the interval arithmetic test on the interval arithmetic version of the box.

- If the box passes the interval arithmetic test, we eliminate it, and switch back to the floating point algorithm.
- If the box fails the interval arithmetic test, we just act as if it failed the corresponding floating point test, and resume the algorithm. We call this case a *mismatch*. It is harmless.

Even though the mismatches are harmless, we prefer to have few mismatches, so that run time for the interval arithmetic version of the code is easier to predict from the run time of the floating point version. There are 4 kinds of potential mismatches, corresponding to the 4 kinds of tests we perform, as discussed in §2.5. The two mismatches that actually arise (or, rather arose) in abundance are the Energy Estimator mismatches and the Redundancy Eliminator mismatches. Once we make our modifications, the

code runs completely without mismatches for the $1/r$ potential and with only a 4 mismatches for the $1/r^2$ potential.

To prevent the Energy Eliminator mismatches, we arrange the floating point eliminator so that a dyadic box passes only if the minimum energy is above $E_0 + 2^{-40}$, where E_0 is the energy of the T.B.P. In this way, the interval versions of the boxes that are actually checked have a bit of a cushion. The reason why this fudge factors does not cause our code to halt is that the inequality $\mathcal{E}(X) - E_0 < 2^{-40}$ only occurs well inside the L^∞ neighborhood of size 2^{-14} about the TBP.

Adding the fudge factor of 2^{-40} makes the floating point test harder to pass, but does not change the validity of the program. Logically, the floating point calculation simply finds a candidate partition of the configuration space, in which each box in the partition passes one of our tests. Adding the fudge factor does change the final partition a bit, but it doesn't destroy the basic property of the partition.

Mismatches occur for the Redundancy Eliminator because we sometimes eliminate configurations where there is an exact equality of coordinates. This equality will fail for the corresponding intervals, because of a tiny overlap. To get around this problem, we associate to each dyadic object a Gaussian integer that represents $2^{25}z$, where z is the center of the object. When we subdivide a dyadic object, we perform the arithmetic on the Gaussian integer exactly, so as to compute the exact value of the centers of the subdivided objects. We never subdivide more than 24 times – and in fact the maximum is about 17 – so we never arrive at a situation where $2^{25}z$ is not an integer. When it comes time to compare the various coordinates of a dyadic object, we actually compare 2^{25} times those coordinates, so that we are working entirely with integers. This lets us make exact comparisons.

There is one more fine point we would like to mention. We want to avoid taking expressions of the form \sqrt{I} , where I is an interval that is too close to 0. If $0 \in I$, then $I_0 < 0$ and $\sqrt{I_0}$ causes an arithmetic error. The only time this issue comes up is in the bounds from Lemma 3.1. The quantity $4 - D^2$ might be close to 0 if D is close to 2. To avoid this problem, we define a new function σ , which has the property $\sigma(I) = 2^{-5}$ if $I_1 < 2^{-10}$ and otherwise $\sigma(I) = \sqrt{I}$. (It never happens that $I_1 > 2^{-10}$ and $I_0 < 0$.) When computing the interval version of the bound in Lemma 3.1, we use σ in place of $\sqrt{\cdot}$. This causes no problem with the proof, because the bound is not as strong when we use σ in place of $\sqrt{\cdot}$.

11 References

[BBCGKS] Brandon Ballinger, Grigoriy Blekherman, Henry Cohn, Noah Giansiracusa, Elizabeth Kelly, Achill Schurmann, *Experimental Study of Energy-Minimizing Point Configurations on Spheres*, arXiv: math/0611451v3, 7 Oct 2008

[C] Harvey Cohn, *Stability Configurations of Electrons on a Sphere*, Mathematical Tables and Other Aids to Computation, Vol 10, No 55, July 1956, pp 117-120.

[CK] Henry Cohn and Abhinav Kumar, *Universally Optimal Distributions of Points on Spheres*, J.A.M.S. **20** (2007) 99-147

[CCD] online website:

<http://www-wales.ch.cam.ac.uk/~wales/CCD/Thomson/table.html>

[DLT] P. D. Dragnev, D. A. Legg, and D. W. Townsend, *Discrete Logarithmic Energy on the Sphere*, Pacific Journal of Mathematics, Volume 207, Number 2 (2002) pp 345–357

[HS], Xiaorong Hou and Junwei Shao, *Spherical Distribution of 5 Points with Maximal Distance Sum*, arXiv:0906.0937v1 [cs.DM] 4 Jun 2009

[I] IEEE Standard for Binary Floating-Point Arithmetic (IEEE Std 754-1985) Institute of Electrical and Electronics Engineers, July 26, 1985

[I2] IEEE Standard for Floating-Point Arithmetic (IEEE Std 754-2008) Institute of Electrical and Electronics Engineers, August 29, 2008.

[RSZ] E. A. Rakhmanoff, E. B. Saff, and Y. M. Zhou, *Electrons on the Sphere*, Computational Methods and Function Theory, R. M. Ali, St. Ruscheweyh, and E. B. Saff, Eds. (1995) pp 111-127

[SK] E. B. Saff and A. B. J. Kuijlaars, *Distributing many points on a Sphere*, Math. Intelligencer, Volume 19, Number 1, December 1997 pp 5-11

[**T**] J. J. Thomson, *On the Structure of the Atom: an Investigation of the Stability of the Periods of Oscillation of a number of Corpuscles arranged at equal intervals around the Circumference of a Circle with Application of the results to the Theory of Atomic Structure*. Philosophical magazine, Series 6, Volume 7, Number 39, pp 237-265, March 1904.

[**W**] S. Wolfram, *The Mathematica Book*, 4th ed. Wolfram Media/Cambridge University Press, Champaign/Cambridge (1999)

[**Wa**] D. Watkins, *Fundamentals of Matrix Calculations*, John Wiley and Sons (2002)

[**Y**], V. A. Yudin, *Minimum potential energy of a point system of charges* (Russian) Diskret. Mat. **4** (1992), 115-121, translation in Discrete Math Appl. **3** (1993) 75-81